https://doi.org/10.5194/egusphere-2025-1091
Preprint. Discussion started: 19 March 2025

Operational and Probabilistic Evaluation of AQMEII-4 Regional Scale Ozone Dry Deposition. Time to Harmonise Our LULC Masks

Ioannis Kioutsioukis[1], Christian Hogrefe[2], Paul .A. Makar[3], Ummugulsum Alyuz[4], Jesse O. Bash[2], Roberto Bellasio[5], Roberto Bianconi[5], Tim Butler[10], Olivia E. Clifton [6,7], Philippe Cheung[3], Alma Hodzic[8], Richard Kranenburg[9], Aura Lupascu[10,11], Kester Momoh[4], Juan Luis Perez- Camaño [12], Jonathan Pleim[2], Young-Hee Ryu[13], Roberto San Jose[12], Donna Schwede[2,14], Ranjeet Sokhi[4], Stefano Galmarini[15,*]

[1] Department of Physics, University of Patras, Patras, Greece
[2] ORD, U.S. EPA, Research Triangle Park, NC, USA
[3] Environment and Climate Change Canada, Toronto, Canada
[4] Centre for Climate Change Research (C3R), University of Hertfordshire, UK
[5] Enviroware srl, Concorezzo, MB, Italy
[6] NASA Goddard Institute for Space Studies, New York, NY, USA
[7] Center for Climate Systems Research, Columbia University, New York, NY, USA
[8] NSF National Center for Atmospheric Research, Boulder, CO, USA
[9] TNO, Utrecht, the Netherlands
[10] Research Institute for Sustainability – Helmholtz Centre Potsdam, Germany
[11] ECMWF, Bonn, Germany
[12] Tech. U. of Madrid (UPM), Madrid, Spain
[13] Yonsei University, Seoul, South Korea
[14] (Retired)
[15] European Commission, Joint Research Centre (JRC), Ispra, Italy

Abstract

We present the collective evaluation of the regional scale models that took part in the fourth edition of the Air Quality Model Evaluation International Initiative (AQMEII). The activity consists of the evaluation and intercomparison of regional scale air quality models run over North American (NA) and European (EU) domains in 2016 (NA) and 2010 (EU). The focus of the paper is ozone deposition. The collective consists in an operational evaluation (Dennis et al., 2010, namely a direct comparison of model-simulated predictions with monitoring data aiming at assessing model performance. Following the AQMEII protocol and Dennis et al. (2010), we also perform a probabilistic evaluation in the form of ensemble analyses and an introductory diagnostic evaluation. The latter, analyses the role of dry deposition in comparison with dynamic and radiative processes and land-use/land-cover types (LULC), in determining surface ozone variability. Important differences are found across deposition results when the same LULC is considered. Furthermore, we found that models use very different LULC masks, thus introducing an additional level of diversity in the model results. The study stresses that, as for other kinds of prior and problem-defining information (emissions, topography or land-water masks), the choice of a LULC mask should not be at modeller's discretion. Furthermore, LULC should be considered as variable to be evaluated in any future model intercomparison, unless set as common input information. The differences in LULC selection can have a substantial impact on model results, making the task of evaluating deposition modules across different regional-scale models very difficult.

*Corresponding author: Dr Stefano Galmarini, European Commission, Joint Research Centre (JRC), Ispra, Italy, email: Stefano.galmarini@ec.europa.eu

https://doi.org/10.5194/egusphere-2025-1091
Preprint. Discussion started: 19 March 2025

1. Introduction

This paper presents the results of the operational and probabilistic evaluation of the regional scale models taking part in the Air Quality Model Evaluation International Initiative phase 4 (AQMEII4) activity. As presented in Galmarini et al. (2021), the AQMEII4 focus is deposition process modelling within regional scale models (AQMEII4-Activity 1) as well as standalone deposition modules (AQMEII4-Activity 2) as detailed in Clifton et al., (2023).

As traditionally done in past editions of the AQMEII activity, and in agreement with the protocol described by Dennis et al. (2010), prior to any detailed analysis of specific process modelling (diagnostic evaluation), a thorough analysis of the overall performance of the model must be conducted via operational and probabilistic evaluation. The scope of such an approach is to verify the positioning of the models participating in AQMEII with respect to observations or any other model simulating the case study or against a multi-model ensemble (Galmarini et al. 2013). Such an analysis has the scope of assisting the interpretation of any other detailed result in this paper or other contribution to the special issue and understanding how the different processes contribute to the model spread. Examples of this approach can be found in Solazzo et al. (2012a and b), Vautard et al. (2012), Im et al. (2015, 2018), Giordano et al. (2015), Brunner et al. (2015), and Kioutsioukis et al. (2016). The evaluation also provides important context for the interpretation of diagnostic results – for example, the contrast in diagnostic comparisons between models with higher and lower evaluation performance helps to identify specific processes which may contribute to the differences (an example of this approach appears in Makar et al. (2024), this issue, for sulphur and nitrogen deposition, and Vivanco et al. (2018)).

Since the operational and probabilistic analysis is instrumental to the interpretation of ozone deposition-related results (the focus of the fourth edition of AQMEII), we shall concentrate on the variables that are directly or indirectly connected to description of deposition processes within the models: namely, atmospheric concentrations, LULC masks and meteorology. A detailed diagnostic analysis of modelled ozone dry deposition can be found in Hogrefe et al. (2025, this issue).

https://doi.org/10.5194/egusphere-2025-1091
Preprint. Discussion started: 19 March 2025

2. Models, domains, and years of consideration

The setup of the AQMEII4 Activity 1 is detailed in Galmarini et al. (2021). In essence, the activity consists of running regional scale models on the North American (NA) and European (EU) domains for the years (2010, 2016) and (2009, 2010) respectively. The models that took part in AQMEII4 are listed in Table 1, where details on the institutions in charge and the cases simulated are also provided. These models and in particular their deposition schemes are described more in detail in Galmarini et al. (2021, this issue) and Makar et al. (2024, this issue). Note that simulations took place with harmonized input emissions fields; all models started with the same anthropogenic, lightning NOx, and forest fire emissions inventory for North America and Europe, respectively (Galmarini et al., 2021), while biogenic emissions and other natural sources of emissions such those of sea-salt particles were carried out as part of internal model processing and should be considered "part of the model" in the analysis that follows.

The analysis described here will focus on two year-long simulations: 2016 for the NA case and 2010 for the EU case. The following aspects will be considered in detail in this paper:

- Analysis of space and/or time averaged ozone concentrations
- Analysis of seasonal, diurnal, and spatial variations of ozone (and to a lesser extent nitric oxide, and nitrogen dioxide concentrations, in order to assist in the ozone analysis).
- Ensemble analysis of modelled ozone concentrations
- The role of variability in effective fluxes for specific pathways in determining the variability of ozone dry deposition flux over different LULC types
- The role of variability in wind speed, mixed layer height, dry deposition, and radiation in determining the variability of ozone concentrations at the surface.

Model values will be evaluated against ozone and precursor concentrations collected by regional operational networks during the year in consideration. More specifically, for North America the monitoring network databases employed included: the U.S. Environmental Protection Agency's Air Quality System (AQS; https://aqs.epa.gov/aqsweb/airdata/download_files.html), the Canadian National Air Pollution Surveillance (NAPS) program (https://www.canada.ca/en/environment-climate-change/services/air-pollution/monitoring-networks-data/national-air-pollution-program.html), and the Canadian National Atmospheric Chemistry database (https://www.canada.ca/en/environment-climate-change/services/air-pollution/monitoring-networks-data/national-atmospheric-chemistry-database.html). For the European case: the European Monitoring and Evaluation Programme

https://doi.org/10.5194/egusphere-2025-1091
Preprint. Discussion started: 19 March 2025

(EMEP; https://www.emep.int/), and the European Air Quality Database (AIRBASE; https://eeadmz1-cws-wp-air02-dev.azurewebsites.net/download-data/).

Given the continental dimension of the two regional domains simulated under AQMEII-4, the latter have been divided into sub-regional domains for analysis. These group portions of the network that share common features such as atmospheric circulation and possible sources of ozone precursors, and also provide continuity with past AQMEII model evaluation phases (Solazzo et al. 2012a and b).

Figure 1 shows the sub-regions selected within the two modelling domains, the corresponding sampling sites and the yearly average measured ozone (a and b). As noted by Solazzo et al (2012a), from the distributions of the pollutants, it is easy to identify the reason for those specific divisions in subdomains. In North America, a longitudinal divide is present between western (R1), central (R2) and eastern parts of the continent while the latter also requires a latitudinal division in two smaller subdomains (R3 and R4) due to the different kind of precursors' distributions and consequent ozone formation potentials. In Europe, the spatial distribution of emitters is different from North America and has greater activity density. There exist areas that require specific attention being almost decoupled from the rest of the continental air shed. These are typically the Iberian Peninsula and southern Mediterranean basin (R4), the Po Valley (R3) and Eastern Europe (R2). These NA and EU analysis sub regions were first defined in Solazzo et al (2012a), though with lesser detail and have been used in subsequent AQMEII analyses (e.g., Hogrefe et al., 2018) with different subdivisions but with the same goal of identifying regions with more homogeneous chemical potentials. For the sake of synthesis and in the absence of direct measurement of ozone deposition, this paper will concentrate exclusively on the model performance with respect to ozone concentrations with a few references to nitrogen oxides to give a more comprehensive sense of the quality of the performance of the individual models and the ensemble.

3. Operational evaluation

3.1 Ozone surface air concentrations

The model performances at continental level and for the whole year are presented in Figure 2-6. For the two continents, the Root Mean Square Error (RMSE) and Mean Bias (MB) are computed from hourly ozone values for the entire year and are shown for each model in Figure 2-6 and Figure 7 for North America, and Figure 8, Figure 9 for Europe. Figure 10 shows the spatial

https://doi.org/10.5194/egusphere-2025-1091
Preprint. Discussion started: 19 March 2025

averages of the results presented in Figures 2 through 5 as box plot diagrams. In general, RMSE for the NA case (and in particular, for two models, namely NA7 (WRF-Chem (UPM)) and NA8 (WRF-Chem (NCAR))) appears to be larger than the EU case. Note that, since ozone values are reported in ppb over NA and ug/m3 over EU, the range of the colour scales over both continents has been set such that the same colours represent the same absolute errors (note the difference in the numerical values for the colour bars for these figures), to account for unit differences and allow for a visual comparison between continents. Most differences from the observations are found in the eastern and south-eastern parts of the NA domain. As can be evinced from the Figure 2-5, three groups of behaviours can be distinguished for the NA case. Relative to the rest of the models, NA1, NA2, NA3 and NA5 (respectively WRF/CMAQ (M3Dry), WRF/CMAQ (STAGE), GEM-MACH (Base), GEM-MACH (Ops)) show low RMSE values and comparable behaviours. NA4 (GEM-MACH (Zhang)) and NA6 (WRF-Chem (RIFS)) show slightly higher errors in the mid to east coast part of the domain whereas NA7 (WRF-Chem (UPM)) and NA8 (WRF-Chem (NCAR)) show markedly higher errors in the mid to eastern part of the domain and along the west coast. Looking at the biases (Figure 3), the analysis presented above is confirmed with some nuances though. In fact, we can see that the grouping can be more refined. A first group is made of the two EPA models NA1 and NA2 (WRF/CMAQ (M3Dry) and WRF/CMAQ (STAGE)) with a widespread overestimation across the continent. NA3 and NA5 (GEM-MACH (Base) and GEM-MACH (Ops)) produce the smallest biases of the group (see also Figure 3 and with a clearer West-East regional separation compared to NA1 and NA2. Finally, NA4, NA6, NA7 and NA8 (GEM-MACH (Zhang), WRF-Chem (RIFS), WRF-Chem (UPM), WRF-Chem (NCAR)) have larger biases, with NA8 having the largest mean bias (MB) of all (Figure 4). This analysis can also help to distinguish the impacts of different deposition modules from the impacts of differences in other aspects of the model on simulated ozone. For example, WRF/CMAQ (M3Dry) and WRF/CMAQ (STAGE) differ only in their dry deposition modules, and the differences between these two simulations are generally smaller than their differences relative to the GEM-MACH and WRF-Chem simulations. On the other hand, the deposition scheme has an important effect when we look at NA4 (GEM-MACH (Zhang)) vs. NA3 (GEM-MACH (Base)). These two models share the same regional scale system but use a different deposition scheme. The effect of the deposition scheme on the ozone concentration is quite remarkable. Recent work emphasizes a substantial effect of the magnitude of deposition velocity on ozone concentration (e.g. Baublitz et al. 2020; Wong et al., 2019; Clifton et al., 2020b), and the results are consistent with those in Clifton et al. (2023) where the individual deposition module performances were evaluated (see discussion below), where larger differences were noted between the Zhang and

https://doi.org/10.5194/egusphere-2025-1091
Preprint. Discussion started: 19 March 2025

Base schemes used in GEM-MACH than between the M3Dry and STAGE schemes used in CMAQ. Comparing NA3 (GEM-MACH (Base)) to NA5 (GEM-MACH (Ops)) reveals the impacts of model configuration and science option choices other than dry deposition, since both simulations use the Wesely scheme but differ in a number of other modelling aspects, as described in more detail in Makar et al. (2024). The relatively low MB for models NA3 and NA5 reflect two different approaches towards reducing ozone biases employed in the two different configurations of the model, with NA3 making use of a canopy shading and turbulence scheme (Makar et al., 2017), and the NA5 scheme making use of an operational configuration in which emitted area-source species are mixed uniformly into the first two model layers rather than input as a flux boundary condition. The effects of model configuration choices are also evident in the results of the three remaining models (WRF-Chem (RIFS), WRF-Chem (UPM), and WRF-Chem (NCAR)) that share the same deposition model and overall model code but utilize different configuration options. These simulations show a consistent overestimation that cannot be attributed clearly to one factor (see also Figure 5). The three implementations are also with respect to three different WRF-Chem version numbers (3.9.1, 4.0.3 and 4.1.2 respectively); the former use the Grell and Devenyi (2002) cumulus parameterization, the latter the Grell and Freitas (2014) parameterization, while both WRF-Chem (RIFS) and WRF-Chem (UCAR) employ the same gas–phase mechanism (Emmons et al., 2010), while that of WRF-Chem (UPM) differs from the other two models. The relatively minor differences between WRF-Chem (UPM) and WRF-Chem (UCAR) may thus reflect differences in the gas-phase chemistry (with the former's mechanism resulting in slightly lower positive bias levels), and the larger differences with the RIFS implementation reflecting differing cloud amounts and hence differing photolysis rates within the two implementations. The large overestimation of ozone by the WRF-Chem (UCAR) configuration may thus be linked to the underestimated precipitation in this model reported elsewhere (e.g. Makar et al. 2024), which also implies smaller cloud amounts and stronger solar radiation.

In Figures 4 and 5, RMSE and MB in Europe are presented, respectively. The errors have more a hot-spot character that is mainly evident in the southern part of the domain and therein at well-recognized critical regions like the Po Valley in the north of Italy, Greece and the Iberian Peninsula. This result is confirmed in the MB plots that also show EU3 (LOTOS/EUROS) as the best-performing model of the four though in many cases underestimating ozone concentration levels. As for the rest of the domain, smaller RMSE values can be noticed throughout the region for all models with the only exception of EU1 (WRF/Chem (RIFS)) and EU4 (WRF/CMAQ (STAGE)) that

https://doi.org/10.5194/egusphere-2025-1091
Preprint. Discussion started: 19 March 2025

show comparatively larger errors, especially in the southern and northern parts of the domain respectively. This behaviour of EU1 and EU4 may be associated with the lower predicted NO_2 and NO concentration for all European sub-regions (see Fig. S4) which in turn may result in positive biases in ozone if the lower NO_x is resulting in reductions in the NOx titration of ozone at night. This effect is apparently exacerbated in the Po Valley area, which is known for high NO_x emission levels. The observational sites in the Scandinavian Peninsula are mainly from the EMEP network which is representative of the remote background whereas the AirBase network rural background sites are more prone to local sources of pollution.

In this case, a model implementation/user effect can be an element of consideration since the EU4 is the same model that is used by EPA in the NA case (NA2), but in this instance run by the University of Hertfordshire. In the implementation of EU4, the primary differences lie in the meteorological model and the MEGAN biogenic emissions input. These variations in meteorological drivers and biogenic emissions can introduce differences, potentially contributing to the observed model biases when compared to other implementations of the same model. However, it should also be noted that the CMAQ simulations in North American (models NA1, NA2, Figure 3) also show positive biases, particularly along the US eastern seaboard. As noted above in the discussion on models NA3 versus NA5, one possible cause for these biases may relate to the extent to which shading and turbulence within the forest canopy is accounted for in these models. The NA3 forest canopy parameterization mentioned above (Makar et al., 2017) is being ported to the CMAQ model in other work (Campbell et al., 2021, Wang et al., 2005); the reduced turbulence and reduced photolysis rates below forest canopies have been shown to result in increases in surface level NOx concentrations, and an extension of the diurnal NOx titration effect further into the daylight hours, significantly reducing surface ozone concentrations. Many of the regions with the highest ozone biases in models EU1, EU2 and EU4 correspond to areas with high forest canopy and leaf area index values, as does the eastern seaboard of the USA and Canada, and the negative biases in EU1 and EU4 for NO and NO_2 are consistent with the absence of the more realistic reduction in thermal diffusivity coefficients and photolysis rates expected under forest canopies (Makar et al., 2017).

From the analysis of NO, NO_2 and O_3 Normalised Root Mean Square Error vs Mean Bias in the soccer plots of Figure S1 in the Supplementary Material (SM, from now on) for the two continents, we notice that the two precursors to ozone show an error smaller than 15% for most models. For the NA case, the ozone soccer plots confirm the grouping of the results qualitatively

https://doi.org/10.5194/egusphere-2025-1091
Preprint. Discussion started: 19 March 2025

derived from the regional analysis of Figure 2. Figure 6 shows that GEM-MACH models NA3 and NA5 have the bias values closest to zero, followed by CMAQ (NA1 and NA2), while CMAQ has the lowest RMSE values, closely followed by the GEM-MACH NA3 and NA5 implementations. Four models show small error (<15%), two with medium (>15% and <20%) and two with high (>20%). The ozone goal plots for the EU (Figure S1) show a statistical tendency to produce smaller errors than the NA case and in particular more coherence between the errors for ozone and its precursors.

The Taylor diagram depicted in Figure S2 in the SM also evaluates the correlation between simulated and observed ozone values. The results show a higher correlation of model predictions with observations in the EU case while the other statistical parameters in the diagram confirm what has been presented in the other plots. The multi model ensemble (MME) is also presented for the two cases, showing in both instances an improved performance with respect to the individual model simulations.

Figure 7 shows a comparison of observed and modelled seasonal and diurnal cycles for ozone, NO and NO_2. These cycles were constructed by averaging the underlying raw hourly data available for the entire year over a given month-of-year or hour-of-day, respectively. At the monthly level, the figure clearly shows that for ozone in NA, almost all models over-estimate the concentration during summer. The multi-model mean fails to reproduce the ozone maximum in April by overshooting by approximately 3 ppb and presenting a maximum in June. This result is driven by 4 out of 8 models (NA4 (GEM-MACH (Zhang)), NA6 (WRF-Chem (RIFS)), NA7 (WRF-Chem (UPM)) and NA8(WRF-Chem (NCAR))). Although slightly overestimating the concentration, two models (NA3 (GEM-MACH (Base)), and NA5 (GEM-MACH (Ops))) manage to reproduce very accurately the seasonal evolution. NA1 and NA2 (WRF/CMAQ (M3Dry) and WRF/CMAQ (STAGE)) capture the trend and seasonality and just slightly overestimate the ozone peak value.

The tendency for overestimating ozone concentration and underestimating NO is also clear from Figure 7 (for NA) and Figure 8(for EU). Figure 7's diurnal variation panels (right hand column) in particular show that the models NA3 and NA5 have the closest values to observations for O_3, NO and NO_2, though all models underestimate the NO_x totals. This is especially evident for NO and NO_2 in the mid-day hours (10 to 18 local time), when the simulated NO and NO_2 values are the closest in the ensemble to the observations. The monthly variation panels (Figure 7 left column) show that the relative impact of the NO_x underestimates is smaller in the summer than in the winter, and models NA3 and NA5 have the closest NO values to observations and slightly

https://doi.org/10.5194/egusphere-2025-1091
Preprint. Discussion started: 19 March 2025

overestimate NO_2 in the summer. Model NA3 includes forest canopy shading effects which reduce vertical turbulence, increase NO_x levels, and decrease photolysis rates below the forest canopy. Model NA3 also includes the effects of vehicle-induced turbulence on NO_x emissions from vehicles (Makar et al., 2021), an effect which results in more efficient dispersion of these emissions out of the surface layer. Model NA5 assumes the area emissions of NO_x are evenly and instantaneously distributed over the first two vertical levels of the model rather than incorporating these emissions as a flux boundary condition on the diffusion equation. At least some of the superior performance for NA3 and NA5 may thus be related to the more rapid rate at which emitted NO and NO_2 are transported upwards out of the model surface, as well as (model NA3) the use of the forest canopy shading parameterization. The ozone deposition velocity used in NA3 and NA5 versus that of NA4 is also a driver for the differences between these models, as noted in Clifton et al. (2023), which noted that NA3 and NA5 shared a scheme which significantly overestimated ozone deposition velocities relative to observations in the summer while providing reasonable estimates during the winter, while the Zhang scheme, used in NA4, showed little seasonal variation (tending to be flat over time, with overestimates during winter, underestimates during summer). It is of note that the models that reproduce the seasonal evolution of ozone most accurately during summer when the rest of the models struggle, have the deposition schemes with the largest positive biases in summertime ozone deposition velocity and the greatest seasonal amplitude (Clifton et al. 2023). This implies (1) that the factors affecting the ozone concentrations have a strong seasonal dependence (models NA4 versus NA3 and NA5), (2) and that while one means of helping achieve that seasonal dependence is through an overestimation of the ozone deposition velocity relative to observations (models NA3 and NA5), (3) *other seasonally dependent process improvements than deposition velocity are required to better simulate ozone* (given that the other models considered here which incorporate more accurate ozone deposition schemes, relative to the observations in Clifton et al. (2023) *also* have high positive biases in parts of NA and EU (Figure 3 and Figure 5). The forest canopy parameterization of Makar et al. (2017) is one such possible means of code improvement[1], in that the associated decreases in near-surface coefficients of

[1] We note that subsequent investigation at ECCC of the GEM-MACH deposition algorithm described in Makar et al. (2018), following the results published in Clifton et al (2023) identified two key errors added to the code in the version subsequent to the code version used in Makar et al (2017). Specifically, the cuticle resistance formula (Makar et al, 2018 equation S.8, Clifton et al (2023) equation (42) made use of Zhang et al (2002) dry cuticle resistance coefficients (rcuti, rlu) which should not have been scaled by inverse leaf area index, and made use of Zhang et al (2002) coefficients for the lower canopy resistance (Makar et al, 2018 equation (S.2), Clifton et al 2023 equation (44) which did not include the required scaling of the coefficients by (LAI^0.25)/(u*)^2. Subsequent to these corrections, a much closer fit to the observations in Clifton et al. (2023) was achieved. (K. Toyota, A. Robichaud, personal communication, 2024).

https://doi.org/10.5194/egusphere-2025-1091
Preprint. Discussion started: 19 March 2025

thermal diffusivity and photolysis rates depend on the leaf-area index of the vegetation, which is highly dependent on seasonality for deciduous forests. The other consideration worth examining is the interdependence between model cloud cover and surface photolysis rates, given the variation between NA WRF-Chem models NA6, NA7, and NA8, where the largest differences in ozone positive bias correspond to the use of differing cloud parameterizations.

For NO and NO_2, the models show seasonal cycles which differ between the models (Figure 7, Figure 8, left-hand columns) versus the observations and between the NA and EU observations. Observed NA ozone peaks in April (month 4, Figure 7 upper left panel), while observed EU ozone peak in July (month 7, Figure 8 upper left panel). As noted above, models NA1, NA2, NA3, and NA5 all capture the NA O_3 seasonality (CMAQ and Base and Ops GEM-MACH configurations) while the WRF-Chem models predict a late summer peak, similar to observations in EU. All models tend to overestimate compared to observed ozone concentrations (exceptions: NA3 and NA5 in April and May, Figure 7, EU2 and EU3 from November to April). All models underestimate wintertime NOx (though NA models NA1, NA2, NA3, NA5, and NA7 have close NO_2 performance to observations from July through October, Figure 7), and EU3 NO values closely match observations, while EU2 NO_2 is biased high relative to observations. All NA models have significant (factor of two or more) negative biases in NO, and the largest seasonal NO_2 negative biases in winter. As a consequence, all NA models strongly underestimate the amplitude of the observed seasonal cycle. Figure 8 also shows that the models with the smallest NO and NO_2 biases (EU2 (WRF-Chem (UPM)) and EU3 (LOTOS/EUROS)) do quite well for O_3, NO and NO_2), and the EU NO and NO_2 biases for these models are in general much smaller than the NA model biases. At the diurnal level (Figure 7, Figure 8 right panels) the results are consistent with what is found at the seasonal level in terms of over- or underestimations. At the diurnal level, EU2 outperforms the others showing a good capacity of catching the average time evolution of the three pollutants.

One overall conclusion from the comparisons with observations for NO, NO_2 and O_3 is that the models which most closely match NO and NO_2 (EU2, EU3) also have the best performance for O_3, that those models with negative biases for NO and NO_2 also have positive biases for O_3, and that the magnitude of the NO_x negative biases is inversely proportional to the magnitude of the O_3 positive biases, for all models. The relative magnitude of the "freshly emitted" component of NO_x (i.e. NO) tends to be underestimated, with the exception of model EU3 (LOTOS/EUROS). These results all point towards *excessive vertical mixing of fresh NO emissions up from the lowest model layer* as a root cause of the model biases in the other models. The reasons for this

https://doi.org/10.5194/egusphere-2025-1091
Preprint. Discussion started: 19 March 2025

conclusion are: (1) the relative fraction of NO_x that is NO will be highest in air dominated by fresh emissions; (2) the relationship between positive ozone biases and negative NO biases indicates that the ozone biases are due to insufficient NO titration; (3) the effect is exacerbated in winter in all NA models and some EU models - a time when the atmosphere tends to be more stable, and photolysis rates in the northern hemisphere are low, both conditions which favour NO_x titration. A secondary cause may be missing NO emissions in the wintertime, though this seems less likely due to the relatively high confidence in mobile emissions and stack which dominate the NO_x emissions totals, and the relatively good performance of EU3 relative to the other EU models when making use of the same emissions inventory.

The monthly averaged ozone, NO and NO_2 concentrations breakdown at the sub regional level are presented in Figures 5 and 6 for NA and EU, respectively. From Figure 9 one can conclude that the major contribution to the domain-wide estimation presented earlier is essentially coming from region R2, R3 and R4 (i.e. the eastern part of the domain) whereas all model results in R1 are rather similar and in agreement with the measurements throughout the year with some models overestimating cold seasons but by a lesser extent than in the other regions. The summertime ozone overestimation over the Eastern U.S. for NA1 and NA2 (WRF/CMAQ (M3Dry) and WRF/CMAQ (STAGE)) is consistent with the findings of Appel et al. (2021). It is also worth noting that all of the NA models (Figure 9) overestimate O_3 in the period from July through September in regions R2, R3, R4; an observed effect largely absent in the EU models (Figure 10). These regional differences will be instrumental to the analysis of deposition processes. The same behaviour observed in sub regions is found at both the seasonal and hourly level. From Figure 10 we can see the situation in Europe, which lacks the large positive biases in the NA simulations.

3.2 Ozone deposition fluxes

We start our examination of O_3 deposition fluxes with the direct comparison of the effective and total fluxes calculated by the models. Effective flux is a convenient way of examining the contribution of the resistances of various pathways towards bulk deposition, taking into account that variability is not only in these resistances but also surface ozone concentrations (Galmarini et al., 2021). The definition of effective fluxes is analogous to the definition of effective conductances (Paulot et al., 2018; Clifton et al., 2020b). Specifically, by definition, the sum of the effective fluxes equals the total ozone dry deposition flux, and this equality is used in the

https://doi.org/10.5194/egusphere-2025-1091
Preprint. Discussion started: 19 March 2025

subsequent analysis. Within AQMEII4, the relevant effective conductances were defined *a priori* and every participating modelling group was requested to determine the combination of all relevant resistances accounted for in their systems, necessary to produce the effective conductances requested. The definitions of the effective conductances, the deposition modelling approaches and the detailed formulation of effective fluxes for each model are presented in Galmarini et al. (2021, this issue). Because effective conductances and ozone concentrations can co-vary on daily timescales, it was important to archive high-frequency effective fluxes; for this same reason, conclusions about drivers of variations in effective fluxes may be distinct from those regarding effective conductances. The analysis of effective and total fluxes is performed only for the grid cells in where all models share the same LULC (for details on the common LULC classifications see Galmarini et al. (2021, this issue)). By restricting the analysis to locations sharing the same characteristics of land use across models, we reduce the impact of LULC variability on the resulting analysis, thus allowing us to compare only the response of models to the different deposition schemes employed for a given LULC. We present model results at grid cells that are covered by at least 85% of respectively, Evergreen Needleleaf Forest (NA: 1544 cells, EU: 2531 cells), Deciduous Broadleaf Forest (NA: 581 cells), Mixed Forest (705 cells), Planted-Cultivated (NA: 6130 cells, EU: 6108 cells), and Urban (32 cells) LULC. In addition, we also define an 'Ozone Receptor' case that corresponds to the grid cells where ozone is monitored at the surface in the two continents (NA 1551 cells, EU 1656) independently from the underlying LULC type, which can therefore be different from model to model.

An important finding is already obtained by simply imposing the selection criterion described above to the data analysed. As can be noted, very few grid cells with the same dominant LULC type are shared by all models for the same continent. This is a clear indication of the fact that individual LULC masks, employed in the models, were obtained from substantially different sources (Table 1). This raises a significant issue with the generation of models examined in AQMEII-4 - whether it is acceptable that the characterisation of the land surface differs so much, when the various masks should be in principle very comparable and given the fact that more recent sources of this information with a high degree of spatial resolution are available. More discussion may be found in Section 5 and in our companion paper (Hogrefe et al., 2025, under review for this issue).

Figures S5 and S6 show seasonal cycles of the total ozone deposition flux and its decomposition into the three different effective fluxes. The pathways represented by these

https://doi.org/10.5194/egusphere-2025-1091
Preprint. Discussion started: 19 March 2025

effective fluxes are (1) lower canopy and soil conductances combined in one factor (LCAN+SOIL) since some models did not distinguish these two terms, (2) cuticular conductance (CUT) and (3) stomatal conductance (ST).

The following features can be appreciated across the model results:

- The magnitude peak of the ozone flux varies considerably from model to model in some cases (NA8) being almost twice that of others (NA4) for the monthly average.
- Typically, the flux is highest during summer and lowest during winter. In some cases, some fluxes show nearly constant values throughout the summer season (NA2, NA3, NA5 and NA7). In others, there is a stronger midsummer peak (NA1, NA4, NA6) in July or August. NA8 shows a double peak shape. Given the deposition scheme is the same in NA8 as NA7 and NA6, this suggests this double peak is either meteorologically driven, or ozone driven.
- In the EU case more homogeneity appears between EU1 and EU2 behaviours while EU4 shows a slightly different performance at this macro level analysis at least.

The breakdown of the contributions of the specific pathways to the total ozone flux does not appear to identify any common behaviour neither across models, nor within the same LULC type nor across time. It is particularly notable that the relative contributions of the different pathways vary between models, (e.g., compare the relative magnitude of stomatal flux in NA1 and NA2, Figure S5(a)). Some models employing the same deposition algorithm nevertheless have different contributions associated with the different pathways (see NA3 versus NA5, which have the same deposition algorithm, yet the soil term dominates in NA3 and the cuticle term dominates in NA5). The latter reflect differences in meteorological drivers; while NA3 and NA5 have the same deposition algorithm, NA3 runs in "aerosol-aware" direct and indirect feedback mode with the aerosols modifying meteorology, and NA5 has no such feedbacks. The differences between these implementations in part are driven by meteorological differences in the deposition velocities themselves, as well as concentration differences arising from other model parameterizations aside from deposition.

We note that an exception to the rule of model differences is for the "planted-cultivated" LULC, where ST and LCAN+SOIL tend to dominate the flux. There is also a clear summer maximum in ST across models (Figure S5e), but the exact seasonality of ST differs significantly between models. LCAN+SOIL tends to have a bi-modal seasonality for this LULC type – with minima during winter and during times of maximum ST. CUT tends to be low – with NA1 and NA2 suggesting slightly

https://doi.org/10.5194/egusphere-2025-1091
Preprint. Discussion started: 19 March 2025

higher values – with weak but noticeable seasonality with a broad growing season peak. To a certain extent, this pattern in seasonal variation in the different pathways and their contribution to the total flux also shows up for deciduous forests (Figure S5c), but less so for CMAQ than for the other models. In general, stomatal flux tends to drive seasonality in the ozone flux, as Clifton et al. (2023) found for ozone deposition velocity at the individual flux sites, but sometimes there is contributing seasonality in non-stomatal flux. The models also all differ in the relative contributions of LCAN+SOIL, CUT, and ST, as also found by Clifton et al. (2023). For example, cuticular flux is very low in some models (e.g., WRF Chem) but a dominant contributor (about 1/3 except over crops) in NA1 and NA2. Perhaps the primary conclusion is that model behaviour can be grouped around the model type. In fact, clear similarities can be found among NA3 and NA5 (GEM-MACH (Base) and GEM-MACH (Ops) for several land-use types), as well as NA6, NA7 and NA8 (WRF-Chem (RIFS), (UPM) and (NCAR) respectively). In the EU case, EU1 and EU2 (both WRF-CHEM) have comparable yearly characteristics, while EU4 (WRF/CMAQ (STAGE) used by the University of Hertfordshire) shares a similar breakdown with NA2 (WRF/CMAQ (STAGE) run by the USA-EPA).

Although relevant for operational evaluation, the analysis in Figures S5 and S6 does not easily reveal the significance of deposition processes and pathways in determining ozone variability across models. Toward this end, hierarchical and variation partitions are considered in Section 5.

4. Probabilistic evaluation

The ensemble analysis described in this section aims to identify the models that contribute to an improved ensemble result and the best combination of models that improves the ensemble skill. Such analysis is part of the probabilistic evaluation described in Dennis et al. (2010) and constitutes one of the four pillars of evaluation defined therein and adopted in the overall AQMEII activity. In past phases of AQMEII, ensemble analysis was also presented as an integral part of the model evaluation (Solazzo et al. 2012a, Solazzo et al. 2012b, Galmarini et al. 2013, Kioutsioukis et al. 2014, Im et al. 2015, Solazzo et al. 2015, Kioutsioukis, et al. 2016, Solazzo et al. 2017, Galmarini et al., 2018). The ensemble mean of the model results has already been presented in the operational analysis. However, identifying which and how many models contribute to improved ensemble results is another question to be addressed in this context. The analysis uses ozone mean concentration measured at the monitoring sites as reference and techniques based on

https://doi.org/10.5194/egusphere-2025-1091
Preprint. Discussion started: 19 March 2025

model combination to determine the optimal results as described in earlier studies (Solazzo et al. 2012a, Solazzo et al. 2012b, Solazzo et al. 2015, Galmarini et al 2013, Kioutsioukis, et al. 2014, Kioutsioukis, et al. 2016, Galmarini et al., 2018).

The skill of an ensemble increases if we combine accurate and diverse models (Kioutsioukis et al., 2014). As shown by Solazzo et al. (2012a) the skill normally reaches a maximum for an ensemble composed of less than half of the available models and then deteriorates when more models are added until reaching an asymptotic value. Given m available models, several combinations of model results in groups of $n \leq m$ can be produced. In this analysis, we aim at identifying the minimum number of models that produce the optimal result and which are the models that produce the highest ensemble skill. We therefore consider all ensembles obtained by combinations of members in a given group constructed from the m models (i.e., a total of $\sum_{n=1}^{m} \binom{m}{n}$ ensembles where $\binom{m}{n}$ represents the combination of n models out of a total of m available). For each combination, we calculate the RMSE, and identify the ensemble with the least error. Note that these ensembles cover the full range of possible combinations from first-order (one model ensemble) to m^{th} order (m = 8 models for NA case and m = 4 models for EU). To avoid the exclusion of yet meaningful results and at the same time to study how the variety of models analysed combines toward those, we also present the results of ensembles with RMSE within 10% of the optimal one. Lastly, we determine the frequency with which each model is selected as part of an optimal ensemble.

In Table 2 the results from NA are presented. The analysis of the 254 ensembles obtained by combining the models in groups of 1, 2, 3 through 8, gives a RMSE ranging from 3.77 to 11.89 ppb. The results from Solazzo et al. (2012a) are confirmed in this study, therefore in the Table 2 we will present only results up to order 4 (i.e. four members in the ensembles) in the NA case, since for higher orders the results only deteriorate. The ensembles with the least error are obtained from the average of two and three models results (i.e. a 2nd and 3rd order ensemble, blue columns). The models that contribute to these two optimal ensembles are WRF/CMAQ (STAGE) and GEM-MACH (Ops) for order 2 and WRF/CMAQ (STAGE), GEM-MACH (Base) and GEM-MACH (ops) for order 3. The second-best ensembles (yellow columns) are also of order 2 and 3 and are composed of GEM-MACH (Base) and GEM-MACH (Ops) results, and WRF/CMAQ (M3Dry), GEM-MACH (Base) and GEM-MACH (Ops), respectively. In particular, it is worth noting that (a) order one features two of the models most present in the ensembles and their individual result is still within 10% of the best higher order ensembles (b) WRF-CMAQ and GEM-MACH are the most

https://doi.org/10.5194/egusphere-2025-1091
Preprint. Discussion started: 19 March 2025

frequent contributors, (c) WRF-Chem versions (RIFS, UPM, NCAR) are never contributing to any ensemble set. We note that both WRF/CMAQ and GEM-MACH (Base and Ops) are used for operational air-quality forecasting in the USA and Canada, respectively, and hence (1) they are frequently evaluated against monitoring data under the principle that new model versions must improve the forecast before replacing old model versions, (2) the ongoing evaluation process will tend to select model configurations with the best performance with respect to ozone concentrations, (3) this ongoing evaluation process is for the model as a whole, while individual processes tend to be evaluated based on other data, and are incorporated into the base code, (4) this process can result in the adoption of processes with compensating errors (c.f. Makar et al. 2014, and note the contrast between deposition velocity performance for NA3, NA5 here versus the deposition velocity performance in Clifton et al., 2023). As new data such as the deposition observations of Clifton et al. (2023) become available, compensating errors come to light, allowing for corrections and updates to the model codes to be carried out.

The EU ensemble (Table 3) has 4 models, which generates 18 ensembles with RMSEs ranging from 7.51 to 14.59 µg/m^3. Four out of the 18 combinations of 2nd, 3rd and 4th order have errors within 10% (yellow column) of the optimal combination generated from LOTOS/EUROS and WRF-Chem (RIFS) for the second order (blue column). No 1st order ensemble has a RMSE smaller than the 2nd order best ensemble, meaning that no individual model run on the EU case performs better than the combination of the two shown in the 2nd order grouping. LOTOS/EUROS is present in all the ensembles created but yet alone is not doing better than when its results are averaged with those of WRF/CMAQ (STAGE). The latter, operated by the University of Hertfordshire for this case study, is present 80% of the time as a contributor to the second- and third-best ensembles. We note that LOTOS/EUROS, like the GEM-MACH and WRF/CMAQ models in NA, provides operational forecasts of O_3, NO_2, and PM_{10}, and hence will likely benefit from ongoing evaluation and selection of process representation that gives the most accurate model results. Since the results of all orders are shown in Table 3 we can see that the conclusion of Solazzo et al. (2012a) is confirmed to the extent that a combination of half of the available members tends to outperform any single model or larger ensemble of results. It should be clear that the number of models is only an indication to the extent to which the combination of specific models allows one to produce the best results with a reduced number of ensemble members.

https://doi.org/10.5194/egusphere-2025-1091
Preprint. Discussion started: 19 March 2025

5. Variance analysis of ozone fluxes and the role of conductances, turbulence, radiation and wind speed to ozone variability on common LULC types

At this stage of the analysis it is important to determine the overall role of deposition and other relevant factors in determining the variability of ozone concentrations at the surface. Having established which grid cells are representing the same LULC characterisation (Section 3.2), we proceed with the analysis of deposition data by identifying a set of parameters that are expected to be relevant in the characterisation of the ozone flux, namely:

- Lower canopy and soil effective flux (LCAN+SOIL) combined as one factor,
- Cuticular effective flux (CUT)
- Stomatal effective flux (ST)

We also identify the factors that are expected to be relevant in the determination of ozone concentration variability at the surface, namely:

- Boundary layer height,
- Solar radiation,
- Wind speed,
- Deposition velocities.

Chemical transformation is a dominant factor in creating ozone variability together with the abundance of ozone precursors. However, it is challenging to represent the influence of these factors through a specific variable, although solar radiation can be viewed as a proxy of photochemical activity. We note that air temperature can also have a significant influence on photochemical formation of ozone, but air temperature will also influence the deposition pathways; the two influences would be difficult to differentiate. Although the analysis will be performed over all the months of the analysed years, the main focus will be around the summer months, when the ozone production and mixing ratios are normally at maximum levels, and when models are performing the worst, at least over NA.

https://doi.org/10.5194/egusphere-2025-1091
Preprint. Discussion started: 19 March 2025

5.1 Relative relevance of pathway fluxes in ozone flux variability

Variation partitioning of a single response variable (Y, e.g. total O_3 flux, or O_3 concentration) is based on the adjusted R^2 in a regression framework (Peres-Neto et al., 2006; Lai et al., 2022). For example, the variation partitioning of O_3 flux between three sets of predictors (X1: LCAN+SOIL, X2: CUT, X3: ST) can be achieved through the estimation of the fractions (represented here by the dummy variables: a, b, c, d, e, f, and g) based on one (X_i), two (X_i, X_j) or three (X_i, X_j, X_k) variables (Figure S7):

(1) fractions based on one variable:

$$[a+d+f+g] = R^2_{Y|X1}$$
$$[b+d+e+g] = R^2_{Y|X2} \quad (1a)$$
$$[c+e+f+g] = R^2_{Y|X3}$$

(2) fractions based on two variables:

$$[a+b+d+e+f+g] = R^2_{Y|(X1,X2)}$$
$$[a+c+d+e+f+g] = R^2_{Y|(X1,X3)} \quad (1b)$$
$$[b+c+d+e+f+g] = R^2_{Y|(X2,X3)}$$

(3) fraction based on all three predictor variables:

$$[a+b+c+d+e+f+g] = R^2_{Y|(X1,X2,X3)} \quad (1c)$$

Y in equations 1 (a,b,c) is the predictor variable in this case ozone flux. From the above expressions, we can estimate the *sole* and *shared* contributions of each predictor. For example, the *sole* and *shared* fraction of variation explained by X_1 are respectively:

$$sole = [a] = [a+b+c+d+e+f+g] - [b+c+d+e+f+g] \quad (2a)$$
$$shared = [d/2 + f/2 + g/3] \quad (2b)$$

where (similarly for the other fractions):

$$[d] = [a+b+c+d+e+f+g] - [c+e+f+g] - [a] - [b]$$

https://doi.org/10.5194/egusphere-2025-1091
Preprint. Discussion started: 19 March 2025

The analysis proceeds by carrying out multiple regressions for the equations 1(a) through 1(c); the values of the left-hand side terms that minimize the differences between left and right-hand sides of the equations are then compared - these provide the relative contribution of the component terms towards the net correlation coefficient between the ozone flux and the three predictors.

For the sake of synthesis in the main paper, we shall present results of the variance decomposition analysis for the two most relevant LULC cases (evergreen needle leaf forest and ozone receptors). The analysis for all other LULC types selected and listed in Section 3.2, is presented in the Supplement.

Figure 11 presents the contribution to the ozone dry deposition flux variability of the three effective fluxes (total or 'sole' plus 'shared': first and third column of plots in each figure) and their decomposition into 'sole' and 'shared' fractions (second and fourth column panels) for all months of 2016 and for the eight models participating in the NA case study for shared cells covered by at least 85% evergreen needle leaf forests.

Considering the first and third columns of Figure 11 (where the sum of Eqs. 2a and 2b is presented) we notice that for all models the fractional contributions to ozone flux variance add up to 1 as expected. For the summer period, we can see that the models can be divided into three main groups. The first group is where stomatal effective fluxes dominate in defining the ozone flux variability (WRF/CMAQ (M3Dry), WRF/CMAQ (STAGE)), a second group where the dominant pathway to ozone flux variability is through the cuticular effective flux (GEM-MACH (Base), GEM-MACH (Ops) and GEM-MACH (Zhang)) and a third group where the main factor is the combined soil and lower canopy effective flux combined (WRF-Chem (RIFS), WRF-Chem (UPM), WRF-Chem (NCAR)). This constitutes a significant result that is also in line with those obtained by Clifton et al. (2023), but extends their finding. For example, Clifton et al. (2023) show that models have very different relative partitioning across effective conductances at individual sites. Our result here suggests that spatial variability in the ozone flux across the same LULC type is mainly determined by different flux pathways. Given the fact that the grid cells selected were dominated by the same land-use type, differences between the three groups can be attributed to substantial differences in the deposition modules, concentration gradients, and meteorology. In the winter and autumn months, the contribution to ozone flux variability is equally distributed across the three pathways for all models for this LULC type. We also note that the seasonal cycle of the "sole" terms varies as a function of model. The stomatal conductance term dominates the CMAQ implementations

https://doi.org/10.5194/egusphere-2025-1091
Preprint. Discussion started: 19 March 2025

(NA1, NA2) in the summertime, while for the GEM-MACH implementations (NA3, NA4, NA5), summertime seasonality is mostly driven by the soil + lower canopy term, while for WRF-Chem implementations (NA6, NA7, NA8), stomatal and soil+lower canopy terms both have a weak maximum in the summer.

In Figure 11 the results of the decomposition obtained according to equation (2) are independently presented (columns 2 and 4). For the sake of presenting the results in a clearer way, the contributions to the variation obtained from equation 2b, are plotted after changing their sign to better distinguish them from the others; but the total sum of the negative and positive values should be 1. This more detailed analysis allows us to verify the previous one with additional details. For example, the predominance of stomatal flux in WRF-CMAQ at the warm season is due to the sole contribution of stomatal flux whereas at the other seasons the shared contributions dominate. For GEM-MACH, the importance of the cuticular flux seen earlier arises from its shared contributions except GEM-MACH (Zhang) where its sole fraction appears equally high throughout the year. Differences between NA3 and NA5 (which share the same deposition code) reflect differences in the driving meteorology: NA3 is a full-feedback version of the model, in which aerosol direct and indirect effects have been incorporated into the model structure - with the result that the model meteorology influencing the deposition flux components differs between the two models (Makar et al., 2015, a,b). Additionally, NA3 uses very different physical parameterizations than NA5, such as a forest canopy parameterization which influences vertical mixing and photolysis rates near the surface (Makar et al., 2017) and a vehicle-induced turbulence parameterization which affects fresh emissions from vehicles on highways (Makar et al., 2021). We note that the WRF-Chem models are also being used in feedback mode and have less variation than the GEM-MACH case, potentially indicating a smaller impact of differing model parameterizations on the feedback portions of the WRF-Chem code. Last, for WRF-Chem, the shared contribution of soil and canopy flux is important all year, but its sole contribution becomes equally high in the warm season.

Figure 12a shows the same analysis for the EU continent where the picture changes completely from NA, indicating very different meteorological drivers between the two regions. This is not unexpected, in that EU meteorology is strongly influenced by the ocean circulation of the Gulf Stream, while the NA meteorology is over a broad region that has a much broader range of conditions in a “continental” climate. In two of the three models (WRF- CHEM), the importance of soil-lower canopy and stomatal effective fluxes in the warm season (mid spring through

https://doi.org/10.5194/egusphere-2025-1091
Preprint. Discussion started: 19 March 2025

October) is due to their shared fractions while the sole contribution of the cuticular effective flux in winter drives the variation of the total O_3 flux. The seasonality of the EU stomatal component is shared with that of NA6, while the EU soil components have a greater degree of seasonality compared to the NA WRF-Chem models. The other model -- EU4 (WRF/CMAQ (STAGE)) -- shows a more even distribution of the stomatal contribution across the year, and a more equal distribution across the three pathways during the year. EU3 is not presented since no data were delivered for effective conductances.

From the figures S8-S10 one can deduce that the rest of the land covers (Deciduous Broadleaf Forest, Mixed Forest, Planted-Cultivated) still exhibit a dominance of stomatal effective flux during the summer. These LULCs all have a significant deciduous component, and the summertime dominance is in part due to the wintertime absence of foliage in the more northerly parts of the model domains. Depending on the model, cuticular and soil are at times the second contributor to variability of ozone flux.

The category 'Ozone Receptor' groups the results at grid cells containing an ozone sampling location regardless of the land cover adopted by individual models (Figure 12b for EU and 9 for NA). It is interesting to notice that the Ozone Receptors case shows a remarkable consistency across models in terms of the contribution of the different effective fluxes and their variability in time, a behaviour not seen when performing this analysis for grid cells dominated by specific LULC types. This can be appreciated from Figure 12 where the evergreen needle-leaf forest case (8a) is presented back-to-back to the ozone receptor case (8b) for the EU domain. There is some disagreement for the EU about the stomatal flux contribution during winter (zero or low) and on the exact partitioning during warm months, but generally all the models show substantial contributions from the stomatal flux, disagreeing on the exact non-stomatal partitioning. The consistency for the Ozone Receptors case is also visible across the continents (Figure 13 for the NA case) where the contribution has a remarkable resemblance across models for seasonality and the partitioning of the ozone flux variance across the effective fluxes, compared to individual land use type values. For the NA case, models suggest moderate to strong contributions for LCAN+SOIL during winter, yet small to moderate contributions during summer; the contribution of cuticular effective flux tends to be constant and moderate throughout the year, with three models (WRF-CHEM) suggesting smaller contributions in winter; with stomatal effective flux making up the difference, roughly a third of the total, but sometimes as low as 10% or as high as 50%.

This result requires a number of important considerations:

https://doi.org/10.5194/egusphere-2025-1091
Preprint. Discussion started: 19 March 2025

1- The remarkable consistency and similarity found among the model results at the receptor locations could be due to the lack of dominance of any specific LULC type at this subset of grid cells considered. This would be in agreement with the fact that the location has presumably been chosen for air quality monitoring activities and is by-design intended to be neutral to any prevailing process, specifically, here, the removal of pollutants from the atmosphere by local processes such as deposition, thus making the monitoring location representative of a particular large region.

2- The variance decomposition into contributions of both *sole* fluxes and *shared* fluxes (columns 2 and 4 of Figure 13 and column 2 in Figure 12b) does not show the same agreement found for the total fluxes (columns 1 and 3 of Figure 13 and column 1 of Figure 12b). This indicates that every deposition model maintains a peculiarity in its behaviour for individual land use types, that is lost in the results when the monitoring station locations are considered. This suggests that while the monitoring station locations show the models perform in a similar fashion for mixtures of LULC types, the model performance for individual land use types (represented by a much smaller number of stations) may differ significantly. Given that model performance is judged using observation station values, this may indicate that deposition algorithms have been inadvertently tuned towards providing similar results in the regions where mixtures of LULC values are present - but require single LULC type stations for the evaluation of individual LULC performance. We note that this tuning is not intentional, but a product of the purpose for which monitoring stations have been set up (e.g. human health impacts, and hence closer to human habitations than remote locations which may have a single LULC) and the availability of infrastructure (roads, electrical power) for station operations. This result underscores the importance of land-use specific deposition sites such as those used in point model deposition velocity analysis in Clifton et al. (2023, this issue) in evaluating deposition algorithms, and suggests that subsets of monitoring network stations located in single LULC types should be identified (or constructed if none are available) in order to further improve model performance within those LULC types. That is, the success of the deposition algorithm has historically tended to be as a component of a regional model and hence will depend on overall model performance and the locations where monitoring station network data are available – hence the deposition algorithm components may be chosen in order to improve performance at the locations where observations are available. The result is that the deposition algorithms are achieving similar results for deposition flux relative to observations – but sometimes via very different pathways, especially across different LULCs. This

https://doi.org/10.5194/egusphere-2025-1091
Preprint. Discussion started: 19 March 2025

is in line with suggestions from recent work examining a single model (Silva and Heald, 2018), a review paper on modelling ozone dry deposition (Clifton et al., 2020a), and the results of the single-point modelling AQMEII Activity 2 paper (Clifton et al., 2023). These findings and the above analysis illustrate a strong need to generate observational datasets which focus on specific deposition components for model evaluation (e.g., as suggested by Clifton et al. 2020a), the need for deposition velocity observation sites to evaluate deposition algorithm performance as a necessary part of deposition algorithm design, and the need, demonstrated above, for monitoring network locations that represent specific LULCs, to improve model performance in regions where one LULC dominates. The current evaluation practice with mixed LULC monitoring stations used for deposition algorithm evaluation prevents progress in algorithm improvement in specific LULCs, and allows for LULC-specific compensating errors to be missed in deposition algorithm development.

3- If (1) and (2) can be confirmed one should consider comparing deposition results obtained at operational monitoring sites with care – the net results of the comparison may be that the regional models and possibly their deposition fluxes agree – on average, for regions with multiple land-use types - but the agreement is the result of regional model evaluation procedures as opposed to mechanistic deposition velocity algorithm evaluation that is LULC-specific. Furthermore, this may give an appearance of agreement among regional models that may be illusory, since in grid cells with shared dominant LULC types more disagreement has been demonstrated in the above analysis. An important implication of this finding is the need to evaluate regional models using both single-land-use and multiple-land-use type stations in the future, and for representation in single-land-use type locations to be a consideration in monitoring network design.

5.2 Non-linear contributions of other factors to the ozone concentration variance

The analysis of the non-linear contributions to the ozone variance has been conducted by introducing other factors considered to be relevant in influencing ozone variability at the surface level, namely: boundary layer height, solar radiation, wind speed, and deposition velocity. In a way, this analysis allows us to determine the role of deposition in relation to other factors influencing the variation of ozone concentrations at the Evergreen Needleleaf Forest cells and therefore estimate its relevance as a driver of ozone variance in a regional scale model. Figure 14 presents the analysis for the NA case while Figure 15 shows results for the EU case.

From Figure 14 we firstly notice that the selected components have a very relevant role in the determination of the surface ozone variance as, overall, they account on average for 60 to 80% of ozone variance. The remaining portion can be attributed to variations in emissions and chemical reactions that cannot easily be represented by a specific variable, or to other factors not considered in this analysis. Throughout the 8 models participating in the NA case study, we can notice the dominance of radiation followed by PBL height and deposition velocity whereas wind speed seems to be relevant throughout the year only for three of the eight (WRF/CMAQ (M3Dry), WRF/CMAQ (STAGE), GEM-MACH (Zhang)). We note that correlation does not necessarily imply causation - the wind speed dependence effects noted here may reflect model dependence on the friction velocity, which can be expressed as a function of the wind speed, logarithmic profile, and surface roughness. The contribution of wind velocity across models is very scattered in time though contributing on average for 30% of the variability. In some models it appears to be among the dominant factors in winter more than in summer (WRF/CMAQ (STAGE), WRF-Chem (RIFS), WRF-Chem (UPM), GEM-MACH (Zhang), WRF/CMAQ (M3Dry)). While WRF-Chem (UPM) uses the CBMZ mechanism (see Makar et al., 2024, this issue), the deposition implementation for CBMZ accounts only for 4 seasons, while the other two WRF-Chem models (RIFS and NCAR) employ the MOZART chemical mechanism, for which the deposition algorithm has tabulated entries on a monthly basis which are used in dry deposition. That is, the WRF-Chem dry deposition implementations which are linked to different gas-phase mechanisms have differing degrees of seasonal resolution. Some of the seasonal differences between NA3 and NA5 implementations of GEM-MACH also relate to seasonality of input information, with NA3 making use of gridded monthly satellite-derived leaf-area index values, and NA5 making use of tabulated 5-season values by LULC. It appears that in North America a seasonality in the contribution of the various components is more evident. The differences between GEM-MACH (Base) and GEM-MACH (Ops) can be attributed at least partially to the meteorology change associated with feedbacks, but also may partially result in the differing seasonality in LAI inputs. The no-feedback model (GEM-MACH (Ops)) has less ozone variability associated with wind speed, and more with solar radiation, compared to the feedback model GEM-MACH (Base); feedbacks exacerbate meteorological variability. GEM-MACH (Base) versus GEM-MACH (Zhang) shows how much the deposition scheme can affect the variability, via the feedbacks: GEM-MACH (Base) and GEM-MACH (Zhang) are otherwise identical models. This quantifies the impact of feedbacks on meteorology and hence deposition velocity variance. WRF-Chem is also a feedback model as well, and the impact of the

https://doi.org/10.5194/egusphere-2025-1091
Preprint. Discussion started: 19 March 2025

feedbacks is showing up as differences in the relative importance of meteorology versus ozone deposition velocity itself between the different implementations.

In EU we see from Figure 15a that the contributions have a greater degree of scatter than for NA. WRF-Chem (UPM) and WRF/Chem (RIFS) share an important contribution of deposition velocity in February and of PBL in April, November and December. Interesting is the fact that across the year the components account for a smaller portion of the total variance (<50%) than in the NA case. This could be due to drastically different conditions and the dominance of variability emissions (and consequently chemistry) on the ozone variability. Each of the models are using different driving meteorology, but the variation in observed conditions across EU may be less than across NA, as noted above. Interesting is the case of March for WRF-Chem (RIFS) where PBL height, solar radiation, wind speed and deposition velocity contribute to less than 5% of the ozone variance. Another difference between the NA and EU case studies is the contribution of deposition compared to the other processes in determining ozone variability. In NA, deposition velocity contributes 10 to 25% to ozone variability during summer and 10 to 50% during winter. In the EU, however, the summer contribution is much lower and in February two models out of four show a 70% contribution.

All these results clearly point toward a relevance of deposition in determining ozone variability and concentrations at the surface and yet they also show that important differences are present in the process description in individual models that can greatly influence the outcome.

When the same analysis is performed at the O_3 Receptor cells, we can clearly demonstrate hypothesis (1) and possibly (2) presented in the previous section. Figures 12 for the NA case and 11b for the EU case show the results for the O_3 receptor cells. The eight models in the NA case clearly show that at those grid cells the contribution of deposition velocity to ozone variability is generally much smaller compared to the results for grid cells with specific common LULC types, for example with respect to Evergreen Needle-leaf Forests. Despite this general trend, NA1, 2, 3 and 5 (WRF/CMAQ (M3Dry), WRF/CMAQ (STAGE), GEM-MACH (Base), GEM-MACH (Ops) respectively) still show that during winter, dry deposition can be a significant contributor to ozone and receptor locations. This result also confirms the hypothesis made at (3) in the previous section; the operational ozone monitoring sites are not suitable for the analysis of deposition results for specific LULC classes. A similar conclusion can be drawn for the EU case (Figure 12b) which is presented back-to-back with the evergreen needle-leaf forest case. To corroborate the last statement, Figure 17 shows a comparison of the fraction of the entire NA common domain

https://doi.org/10.5194/egusphere-2025-1091
Preprint. Discussion started: 19 March 2025

(excluding grid cells dominated by water, i.e. water fraction > 0.5) covered by each LU type to the LU distribution of all grid cells corresponding to O_3 receptor locations (EU results are shown as Figure S10 in the SM). As can be noticed, existing O_3 receptor locations are characterised mainly by Planted/Cultivated, Shrub land and urban LULC with a 10% coverage of deciduous broadleaf forest (Figure 17b). At these locations all models appear to have the same distribution of the main LULC type apart from Shrubland (NA3, 4 and 5 20% more abundant) and Planted/Cultivated (same models 10 % less abundant). However, the distribution of LULC from the overall NA common model domain (Figure 17a) demonstrates that the current receptor site LULC poorly represent the relative amount of land use occurring throughout the domain, with, for example, much higher Evergreen Needleleaf and Grassland fractions, and much lower urban land use LULC in the all-domain data of Figure 17a compared to the observing station values of Figure 17b.

In this respect, it is important also to notice that in spite of the formal differences among deposition modules (Galmarini et al., 2021), in conditions of uniform LU characteristics and dominance of urban and Planted/Cultivated LULC types, the models tend to produce comparable results in terms of contributors to ozone variability. This result further underlines the importance of a correct and uniform characterization of the both the input LULC data and the extent to which monitoring station data reflect LULC across the domain, both of which are driving factors in determining the differences among deposition modules.

6. Conclusions

An operational evaluation has been conducted on the models that took part to the AQMEII4 activity (Galmarini et al., 2021). A total of 12 models were analysed, 8 of which were run on a NA continental air quality simulation of the year 2016 and the rest were run over Europe for the year 2010. The scope of the evaluation is to determine the level of agreement of the models against available measurements and how they compare with one another. This is normally referred to as operational evaluation and according to Dennis et al, (2010) is the first necessary step prior to any more detailed evaluation or inter-comparison of model results. The focus of the fourth phase of AQMEII is the analysis of the performance of deposition schemes in regional scale models, therefore the operational evaluation has been performed having that goal in mind. Ozone deposition, in particular, is the focus of this analysis. Ozone average annual concentration errors ranged between 10 and 30% in NA and between 10 and 15% in EU. Errors for NO and NO_2 were

https://doi.org/10.5194/egusphere-2025-1091
Preprint. Discussion started: 19 March 2025

on the order of 5-10% and 10-15% respectively in NA and 15% for both pollutants in EU. The sub regional analysis confirmed these findings, with the expected sub regional variability related to different emission patterns. The models can be distinctively grouped by performance with WRF/CMAQ (M3Dry), WRF/CMAQ (STAGE), GEM-MACH (Base) and GEM-MACH(Ops) showing a better overall capacity of predicting ozone concentrations in NA followed by GEM-MACH (Zhang) and WRF-Chem (RIFS), while WRF-Chem (RIFS) and WRF-Chem (NCAR) show larger errors throughout the year and the domain. In the EU case LOTOS/EUROS outperforms the two WRF-Chem versions (RIFS and UPM) and WRF/CMAQ (STAGE). This result is also very evident from the probabilistic analysis where all combinations of possible ensembles were calculated, and reflects the models which undergo regular operational evaluation against observations.

As far as the deposition is concerned, an analysis of the variance contribution of the different pathways to the variance of the overall ozone deposition fluxes has been conducted. All cells covered with at least 85% of the same land-use types were considered in this analysis. Across grid cells containing mostly needleleaf forests over the USA, the main example used in our study, the analysis shows the mixed response of the various deposition schemes adopted in the regional scale models; one group of models shows a prevailing contribution of the stomatal effective flux in determining spatial ozone flux variability, one shows the three pathways contribute rather equally, and the last group of models for which the lower canopy and soil effective flux is the prevailing contributor. Thus, models are simulating very different drivers of ozone flux variability in space, even for the same land use type. The contribution to ozone variability of wind speed, deposition velocity, solar radiation and boundary layer height was also investigated.

When the above-mentioned analysis was also performed for all grid cells where ozone monitors were present regardless of the LULC type, a remarkable result was found. Regardless of the EU or NA case considered, all the differences among models found for specific LULC types largely disappeared, showing a more uniform behaviour across models. This aspect was demonstrated to be attributable to a minor contribution of deposition at those sites in determining the ozone variability when compared with other factors. Other factors contributing to this behaviour are the presence of predominant LULC types for which deposition is relatively low and the uniform distribution of those types and other LULC types across the models at the observation station locations.

https://doi.org/10.5194/egusphere-2025-1091
Preprint. Discussion started: 19 March 2025

This result allows us to present important conclusions. The first conclusion is that the evaluation of deposition processes should not be conducted only at operational ozone monitoring sites. The latter's characteristics are selected due to other considerations aside from deposition velocity evaluation, and may be unsuitable for deposition algorithm evaluation, leading to an illusory agreement of models as far as deposition is concerned. Therefore, specific sites with a predominance of LULCs with higher deposition should be selected from existing monitoring stations, or added to existing monitoring networks, for deposition-focused model evaluation. The second conclusion is a recurring theme throughout AQMEII4 regional modelling studies to date (e.g., Hogrefe et al, 2025, Makar et al., 2024), namely the necessity for a harmonisation of LULC data across regional scale air quality models, as a large diversity in the characterization of the surface is still present among all models, and this diversity has a significant impact on model performance. Considering the existence of detailed information in space and time of LULC (e.g., Copernicus Land Monitoring services, USGS, LandSat, etc.), we find the lack of agreement between models on the input land use data of great concern and anachronistic. Any interpretation of the behaviour of deposition schemes will be impaired by the lack of agreement of LULC masks, and will inevitably include an inherent uncertainty difficult to quantify. The present situation is comparable to a hypothetical one where models use different topographies or terrain elevations to the extent of including (excluding) specific reliefs or mountain ranges in (from) the domain. If there is an ambition to improve the performance of regional scale models in terms of deposition processes (effectively a sink in the concentration budget), the selection of up-to-date and common LULC data is a fundamental and necessary prerequisite. Considering the advances in the characterisation of land surface at very high spatial and temporal resolutions (metre scale), such effort cannot be further delayed and should be taken on prior to any new model evaluation or intercomparison of deposition processes.

Disclaimer**:** The views expressed in this article are those of the authors and do not necessarily represent the views or policies of the U.S. Environmental Protection Agency.

Competing Interests: One of the co-authors (SG) is a member of the editorial board of Atmospheric Chemistry and Physics Author

Contributions: SG, IK, CH and PAM: study design. SG: manuscript writing. IK: analyses and plots. PAM, CH, OEC, SG: AQMEII4 steering committee coordination. PAM and PC: GEM-MACH simulations. CH, JOB: CMAQ-

https://doi.org/10.5194/egusphere-2025-1091
Preprint. Discussion started: 19 March 2025

M3Dry, CMAQ-STAGE simulations. RB and RB: ENSEMBLE system for submission of model output, monitoring data selection and organization. AL and TB: WRF-Chem (IASS) simulations. AH and YHC: WRF-Chem (UCAR) simulations, comments on manuscript. OEC and DS: comments on manuscript. RK: LOTOS-EUROS simulations. JLPC and RSJ: WRF-Chem (UPM) simulations, reanalysis of WRF-Chem output. UA and RS: WRF-CMAQ (UH) simulations.

References

Appel, K. W., Bash, J. O., Fahey, K. M., Foley, K. M., Gilliam, R. C., Hogrefe, C., Hutzell, W. T., Kang, D., Mathur, R., Murphy, B. N., Napelenok, S. L., Nolte, C. G., Pleim, J. E., Pouliot, G. A., Pye, H. O. T., Ran, L., Roselle, S. J., Sarwar, G., Schwede, D. B., Sidi, F. I., Spero, T. L., and Wong, D. C.: The Community Multiscale Air Quality (CMAQ) model versions 5.3 and 5.3.1: system updates and evaluation, Geosci. Model Dev., 14, 2867–2897, https://doi.org/10.5194/gmd-14-2867-2021, 2021

Baublitz, C. B., Fiore, A. M., Clifton, O. E., Mao, J., Li, J., Correa, G., Westervelt, D. M., Horowitz, L. W., Paulot, F., and Williams, A. P.: Sensitivity of Tropospheric Ozone Over the Southeast USA to Dry Deposition, Geophys. Res. Lett., 47, e2020GL087158, https://doi.org/10.1029/2020GL087158, 2020.

Brunner D., N. Savage, O. Jorba, B. Eder, L. Giordano, A. Badia, A. Balzarini, R. Baró, R. Bianconi, C. Chemel, G. Curci, R. Forkel, P. Jiménez-Guerrero, M. Hirtl, A. Hodzic, L. Honzak, U. Im, C. Knote, P. Makar, A. Manders-Groot, E. van Meijgaard, L. Neal, J. L. Pérez, G. Pirovano, R. San Jose, W. Schröder, R. S. Sokhi, D. Syrakov, A. Torian, P. Tuccella, J.Werhahn, R. Wolke, K. Yahya, R. Zabkar, Y. Zhang, C. Hogrefe, S. Galmarini, Comparative analysis of meteorological performance of coupled chemistry-meteorology models in the context of AQMEII phase 2, Atmospheric Environment, Volume 115, 2015, Pages 470-498, ISSN 1352-2310 https://doi.org/10.1016/j.atmosenv.2014.12.032.

Campbell, P.C., Tang, Y., Lee, P., Baker, B., Tong, D., Saylor, R., Stein, A., Huang, J., Huang, H-C., Strobach, E., McQueen, J., Stajner, I., Sims, J., Tirado-Delgado, J., Jung, Y., Spero, T.L., Gilliam, R.C., Neish, M., and Makar, P.: The national air-quality forecast capability using the NOAA global forecast system: model developments and community applications, CMAS conference presentation, 16pp, https://www.cmascenter.org/conference/2021/slides/campbell-naq-forecast-capability-2021.pdf , 2021.

Clifton, O. E., Fiore, A. M., Massman, W. J., Baublitz, C. B., Coyle, M., Emberson, L., Fares, S., Farmer, D. K., Gentine, P., Gerosa, G., Guenther, A. B., Helmig, D., Lombardozzi, D. L., Munger, J. W., Patton, E. G., Pusede, S. E., Schwede, D. B., Silva, S. J., Sörgel, M., Steiner, A. L., and Tai, A. P. K.: Dry deposition of ozone over land: processes, measurement, and modeling, Rev. Geophys., 58, e2019RG000670, https://doi.org/10.1029/2019RG000670, 2020a.

Clifton, O. E., Paulot, F., Fiore, A. M., Horowitz, L. W., Correa, G., Baublitz, C. B., Fares, S., Goded, I., Goldstein, A. H., Gruening, C., Hogg, A. J., Loubet, B., Mammarella, I., Munger, J. W., Neil, L., Stella, P., Uddling, J., Vesala T., and Weng, E.: Influence of dynamic ozone dry deposition on ozone pollution, J. Geophys. Res.-Atmos., 125, e2020JD032398, https://doi.org/10.1029/2020JD032398, 2020b.

Clifton, O. E., Schwede, D., Hogrefe, C., Bash, J. O., Bland, S., Cheung, P., Coyle, M., Emberson, L., Flemming, J., Fredj, E., Galmarini, S., Ganzeveld, L., Gazetas, O., Goded, I., Holmes, C. D., Horváth, L., Huijnen, V., Li, Q., Makar, P. A., Mammarella, I., Manca, G., Munger, J. W., Pérez-Camanyo, J. L., Pleim, J., Ran, L., San Jose, R., Silva, S. J., Staebler, R., Sun, S., Tai, A. P. K., Tas, E., Vesala, T., Weidinger, T., Wu, Z., and Zhang, L.: A single-point modeling approach for the intercomparison and evaluation of ozone dry deposition across chemical transport models (Activity 2 of AQMEII4), Atmos. Chem. Phys., 23, 9911–9961, https://doi.org/10.5194/acp-23-9911-2023, 2023.

Dennis, R., Fox, T., Fuentes, M. et al. A framework for evaluating regional-scale numerical photochemical modeling systems. Environ Fluid Mech 10, 471–489 (2010). https://doi.org/10.1007/s10652-009-9163-2

Emmons, L. K., Walters, S., Hess, P. G., Lamarque, J.-F., Pfister, G. G., Fillmore, D., Granier, C., Guenther, A., Kinnison, D., Laepple, T., Orlando, J., Tie, X., Tyndall, G., Wiedinmyer, C., Baughcum, S. L., and Kloster, S.: Description and evaluation of the Model for Ozone and Related chemical Tracers, version 4 (MOZART-4), Geosci. CMAQ (Hertfordshire)ev., 3, 43–67, 2010. https://doi.org/10.5194/gmd-3-43-2010

Galmarini, S., Makar, P., Clifton, O. E., Hogrefe, C., Bash, J. O., Bellasio, R., Bianconi, R., Bieser, J., Butler, T., Ducker, J., Flemming, J., Hodzic, A., Holmes, C. D., Kioutsioukis, I., Kranenburg, R., Lupascu, A., Perez-Camanyo, J. L., Pleim, J., Ryu, Y.-H., San Jose, R., Schwede, D., Silva, S., and Wolke, R.: Technical note: AQMEII4 Activity 1: evaluation of wet and dry deposition schemes as an integral part of regional-scale air quality models, Atmos. Chem. Phys., 21, 15663–15697, https://doi.org/10.5194/acp-21-15663-2021, 2021.

Galmarini S., Kioutsioukis I., Solazzo E., Alyuz U., Balzarini A., Bellasio R., Benedictow A.M.K., Bianconi R., Bieser J., Brandt J., Christensen J.H., Colette A., Curci G., Davila Y., Dong X., Flemming J., Francis X., Fraser A., Fu J., Henze D.K, Hogrefe C., Im U., Garcia Vivanco M., Jiménez-Guerrero P., Eiof Jonson J-.E., Kitwiroon N., Manders A., Mathur R., Palacios-Peña L., Pirovano G., Pozzoli L., Prank M., Schultz M., Sokhi R., Sudo K., Tuccella P., Takemura T., Sekiya T., and Unal A., Two-scale multi-model ensemble: is a hybrid ensemble of opportunity telling us more? Atmos. Chem. Phys., 18, 8727–8744, https://doi.org/10.5194/acp-18-8727-2018, 2018.

Galmarini, S., Kioutsioukis, I., and Solazzo, E.: *E pluribus unum*: ensemble air quality predictions, Atmos. Chem. Phys., 13, 7153–7182, https://doi.org/10.5194/acp-13-7153-2013, 2013.

Giordano, L., Brunner, D., Flemming, J., Hogrefe, C., Im, U., Bianconi, R., , A. Badia, A. Balzarini, R. Baró, C. Chemel, G. Curci, R. Forkel, P. Jiménez-Guerrero, M. Hirtl, A. Hodzic, L. Honzak, O. Jorba, C. Knote, J.J.P. Kuenen, P.A. Makar, A. Manders-Groot, L. Neal, J.L. Pérez, G. Pirovano, G. Pouliot, R. San José, N. Savage, W. Schröder, R.S. Sokhi, D. Syrakov, A. Torian, P. Tuccella, J. Werhahn, R. Wolke, K. Yahya, R. Žabkar, Y. Zhang,… Galmarini, S. (2015). Assessment of

https://doi.org/10.5194/egusphere-2025-1091
Preprint. Discussion started: 19 March 2025

the MACC reanalysis and its influence as chemical boundary conditions for regional air quality modeling in AQMEII-2. Atmospheric Environment, 115, 371-388. doi:10.1016/j.atmosenv.2015.02.034

Grell, G. A. and Freitas, S. R.: A scale and aerosol aware stochastic convective parameterization for weather and air quality modeling, Atmos. Chem. Phys., 14, 5233–5250, https://doi.org/10.5194/acp-14-5233-2014, 2014.

Grell, G. A., and D. Dévényi, A generalized approach to parameterizing convection combining ensemble and data assimilation techniques, Geophys. Res. Lett., 29(14), doi:10.1029/2002GL015311, 2002.

Hogrefe, C., Liu, P., Pouliot, G., Mathur, R., Roselle, S., Flemming, J., Lin, M., and Park, R. J.: Impacts of different characterizations of large-scale background on simulated regional-scale ozone over the continental United States, Atmos. Chem. Phys., 18, 3839–3864, https://doi.org/10.5194/acp-18-3839-2018, 2018.

Hogrefe, C., Bash, J. O., Pleim, J. E., Schwede, D. B., Gilliam, R. C., Foley, K. M., Appel, K. W., and Mathur, R.: An analysis of CMAQ gas-phase dry deposition over North America through grid-scale and LULC-specific diagnostics in the context of AQMEII4, Atmos. Chem. Phys., 23, 8119–8147, https://doi.org/10.5194/acp-23-8119-2023, 2023.

Hogrefe C., Galmarini S., Makar P. A. , Kioutsioukis I., Clifton O. E., Alyuz U., Bash J. O., Bellasio R. , Bianconi R. , Butler T., Cheung P., Hodzic A., Kranenburg R., Lupascu A., Momoh K., Perez-Camanyo J.-L., Pleim J.E., Ryu Y.-H. , San Jose R. , Schaap M., Schwede D. B., and Sokhi R., A Diagnostic Intercomparison of Modeled Ozone Dry Deposition Over North America and Europe Using AQMEII4 Regional-Scale Simulations, egusphere-2025-225, Under review, this issue, 2005

Im U., Bianconi R., Solazzo E., Kioutsioukis I., Badia A., Balzarini A., Baró R., Bellasio R., Brunner D., Chemel C., Curci G., Flemming J., Forkel R., Giordano L., Jiménez-Guerrero P., Hirtl M., Hodzic A., Honzak L., Jorba O., Knote C., Kuenen J.J.P., A. Makar P., Manders-Groot A., Neal L., Pérez J.L., Pirovano G., Pouliot G, San Jose R., Savage N., Schroder W., Sokhi R.S., Syrakov D., Torian A., Tuccella P., Werhahn J., Wolke R., Yahya K., Zabkar R., Zhang Y., Zhang J., Hogrefe C., Galmarini S., Evaluation of operational on-line-coupled regional air quality models over Europe and North America in the context of AQMEII phase 2. Part I: Ozone, Atmospheric Environment, Volume 115, 2015, Pages 404-420, ISSN 1352-2310, doi: 10.1016/j.atmosenv.2014.09.042.

Im, U., Christensen, J. H., Geels, C., Hansen, K. M., Brandt, J., Solazzo, E., Alyuz, U., Balzarini, A., Baro, R., Bellasio, R., Bianconi, R., Bieser, J., Colette, A., Curci, G., Farrow, A., Flemming, J., Fraser, A., Jimenez-Guerrero, P., Kitwiroon, N., Liu, P., Nopmongcol, U., Palacios-Peña, L., Pirovano, G., Pozzoli, L., Prank, M., Rose, R., Sokhi, R., Tuccella, P., Unal, A., Vivanco, M. G., Yarwood, G., Hogrefe, C., and Galmarini, S.: Influence of anthropogenic emissions and boundary conditions on multi-model simulations of major air pollutants over Europe and

https://doi.org/10.5194/egusphere-2025-1091
Preprint. Discussion started: 19 March 2025

North America in the framework of AQMEII3, Atmos. Chem. Phys., 18, 8929–8952, https://doi.org/10.5194/acp-18-8929-2018, 2018.

Kioutsioukis, I. and Galmarini, S.: *De praeceptis ferendis*: good practice in multi-model ensembles, Atmos. Chem. Phys., 14, 11791–11815, https://doi.org/10.5194/acp-14-11791-2014, 2014.

Kioutsioukis, I., Im, U., Solazzo, E., Bianconi, R., Badia, A., Balzarini, A., Baró, R., Bellasio, R., Brunner, D., Chemel, C., Curci, G., van der Gon, H. D., Flemming, J., Forkel, R., Giordano, L., Jiménez-Guerrero, P., Hirtl, M., Jorba, O., Manders-Groot, A., Neal, L., Pérez, J. L., Pirovano, G., San Jose, R., Savage, N., Schroder, W., Sokhi, R. S., Syrakov, D., Tuccella, P., Werhahn, J., Wolke, R., Hogrefe, C., and Galmarini, S.: Insights into the deterministic skill of air quality ensembles from the analysis of AQMEII data, Atmos. Chem. Phys., 16, 15629–15652, https://doi.org/10.5194/acp-16-15629-2016, 2016.

Lai J., Y. Zou, J. Zhang & P. Peres-Neto. 2022. Generalizing hierarchical and variation partitioning in multiple regression and canonical analysis using the rdacca.hp R package. Methods in Ecology and Evolution, 13: 782–788.

Makar, P. A., Cheung, P., Hogrefe, C., Akingunola, A., Alyuz-Ozdemir, U., Bash, J. O., Bell, M. D., Bellasio, R., Bianconi, R., Butler, T., Cathcart, H., Clifton, O. E., Hodzic, A., Koutsioukis, I., Kranenburg, R., Lupascu, A., Lynch, J. A., Momoh, K., Perez-Camanyo, J. L., Pleim, J., Ryu, Y.-H., San Jose, R., Schwede, D., Scheuschner, T., Shephard, M., Sokhi, R., and Galmarini, S.: Critical Load Exceedances for North America and Europe using an Ensemble of Models and an Investigation of Causes for Environmental Impact Estimate Variability: An AQMEII4 Study, EGUsphere [preprint], https://doi.org/10.5194/egusphere-2024-2226, 2024.

Makar, P.A., Stroud, C., Akingunola, A., Zhang, J., Ren, S., Cheung, P., and Zheng, Q., Vehicle-induced turbulence and atmospheric pollution, Atm. Chem. Phys., 21, 12291–12316, https://doi.org/10.5194/acp-21-12291-2021, 2021.

Makar, P.A., Staebler, R., Akingunola, A., Zhang, J., McLinden, C., Kharol, S.K., Pabla, B., Cheung, P., Zheng, Q., The effects of forest canopy shading and turbulence on boundary layer ozone. Nat Commun 8, 15243, 2017. https://doi.org/10.1038/ncomms15243

Makar, P.A., Gong, W., Hogrefe, C., Zhang, Y., Curci, G., Žabkar, R., Milbrandt, J., Im, U., Balzarini, A., Baró, R. , Bianconi, R., Cheung, P., Forkel, R., Gravel, S., Hirtl, M., Honzak, L., Hou, A., Jiménez-Guerrero, P., Langer, M., Moran, M.D., Pabla, B., Pérez, J.L., Pirovano, G., San José, R., Tuccella, P., Werhahn, J., Zhang, J., Galmarini, S., Feedbacks between air pollution and weather, part 2: Effects on chemistry, Atm. Env., 115, 499-526, 2015b. https://doi.org/10.1016/j.atmosenv.2014.10.021

Makar, P.A., Gong, W., Milbrandt, J., Hogrefe, C., Zhang, Y., Curci, G., Žabkar, R., Im, U. Balzarini, A., Baro, R., Bianconi, R., Cheung, P., Forkel, R., Gravel, S., Hirtl, M., Honzak, L., Hou, A., Jiménez-Guerrero, P., Langer, M., Moran, M.D., Pabla, B., Pérez, J.L., Pirovano, G., San José, R., Tuccella, P., Werhahn, J., Zhang, J., and Galmarini, S., Feedbacks between air pollution and weather, Part 1: Effects on weather, Atm. Env., 115, 442-469, 2015a. https://doi.org/10.1016/j.atmosenv.2014.12.003

https://doi.org/10.5194/egusphere-2025-1091
Preprint. Discussion started: 19 March 2025

Makar, P.A., Nissen, R., Teakles, A., Zhang, J., Zheng, Q., Moran, M.D., Yau, H., diCenzo, C., Turbulent transport, emissions, and the role of compensating errors in chemical transport models, Geosci. Model Dev., 7, 1001-1024, 2014. https://doi.org/10.5194/gmd-7-1001-2014.

Makar, P. A., Akingunola, A., Aherne, J., Cole, A. S., Aklilu, Y.-A., Zhang, J., Wong, I., Hayden, K., Li, S.-M., Kirk, J., Scott, K., Moran, M. D., Robichaud, A., Cathcart, H., Baratzedah, P., Pabla, B., Cheung, P., Zheng, Q., and Jeffries, D. S.: Estimates of exceedances of critical loads for acidifying deposition in Alberta and Saskatchewan, Atmos. Chem. Phys., 18, 9897–9927, https://doi.org/10.5194/acp-18-9897-2018, 2018.

Paulot, F., Malyshev, S., Nguyen, T., Crounse, J. D., Shevliakova, E., and Horowitz, L. W.: Representing sub-grid scale variations in nitrogen deposition associated with land use in a global Earth system model: implications for present and future nitrogen deposition fluxes over North America, Atmos. Chem. Phys., 18, 17963–17978, https://doi.org/10.5194/acp-18-17963-2018, 2018. Peres-- Neto, P. R., Legendre, P., Dray, S., & Borcard, D. (2006). Variation partitioning of species data matrices: Estimation and comparison of fractions. Ecology, 87, 2614–- 2625.

Silva, S. J. and Heald, C. L.: Investigating dry deposition of ozone to vegetation, J. Geophys. Res.-Atmos., 123, 559–573, https://doi.org/10.1002/2017JD027278, 2018.

Solazzo E., Bianconi, R., Pirovano, G., Matthias, V., Vautard, R.,.D., Appel, K.W., Bessagnet, B., Brandt, J., Christensen, J. H., Chemel, C., Coll, I., Ferreira, J., Forkel, R., Francis, X.V., Grell, G., Grossi, P., Hansen, A.B., Miranda, A.I., Nopmongcol, U., Prank, M., Sartelet, K.N., Schaap, M., Silve, J.D.r, Sokhi, R.S., Vira, J., Werhahn, J., Wolke, R., Yarwood, G., Zhang, J., Rao, S.T., Galmarini, S., Operational model evaluation for particulate matter in Europe and North America in the context of AQMEII, Atmospheric Environment, Volume 53, 2012a, Pages 75-92, ISSN 1352-2310, doi: 10.1016/j.atmosenv.2012.02.045.

Solazzo E., Bianconi R., Vautard R., Appel K.W., Moran M.D., Bessagnet B, Brandt J., Christensen J.H., Chemel C., Coll I., van der Gon H.D., Ferreira J., Forkel R., Francis X.V., Grell G., Grossi P., Hansen .B., Jeričević A., Kraljević L., Miranda .I., Nopmongcol U., Pirovano G., Prank M., Riccio A., Sartelet K.N., Schaap M., Silver J.D., Sokhi R.S., Vira J., Werhahn J., Wolke R., Yarwood G., Rao S.T., Galmarini S., Model evaluation and ensemble modelling of surface-level ozone in Europe and North America in the context of AQMEII, Atmospheric Environment, Volume 53, 2012b, Pages 60-74, ISSN 1352-2310, doi: 10.1016/j.atmosenv.2012.01.003.

Solazzo, E., Bianconi, R., Hogrefe, C., Curci, G., Tuccella, P., Alyuz, U., Balzarini, A., Baró, R., Bellasio, R., Bieser, J., Brandt, J., Christensen, J. H., Colette, A., Francis, X., Fraser, A., Vivanco, M. G., Jiménez-Guerrero, P., Im, U., Manders, A., Nopmongcol, U., Kitwiroon, N., Pirovano, G., Pozzoli, L., Prank, M., Sokhi, R. S., Unal, A., Yarwood, G., and Galmarini, S.: Evaluation and error apportionment of an ensemble of atmospheric chemistry transport modeling systems: multivariable temporal and spatial breakdown, Atmos. Chem. Phys., 17, 3001–3054, https://doi.org/10.5194/acp-17-3001-2017, 2017.

Solazzo, E., Bianconi, R., Pirovano, G., Moran, M. D., Vautard, R., Hogrefe, C., Appel, K. W., Matthias, V., Grossi, P., Bessagnet, B., Brandt, J., Chemel, C., Christensen, J. H., Forkel, R., Francis, X. V., Hansen, A. B., McKeen, S., Nopmongcol, U., Prank, M., Sartelet, K. N., Segers, A., Silver, J. D., Yarwood, G., Werhahn, J., Zhang, J., Rao, S. T., and Galmarini, S.: Evaluating the capability of regional-scale air quality models to capture the vertical distribution of pollutants, Geosci. Model Dev., 6, 791–818, https://doi.org/10.5194/gmd-6-791-2013, 2013.

Solazzo, E., Riccio, A., Kioutsioukis, I., and Galmarini, S.: Pauci ex tanto numero: reduce redundancy in multi-model ensembles, Atmos. Chem. Phys., 13, 8315–8333, https://doi.org/10.5194/acp-13-8315-2013, 2013.

Vivanco M. G., Mark R. Theobald, Héctor García-Gómez, Juan Luis Garrido, Marje Prank, Wenche Aas, Mario Adani, Ummugulsum Alyuz, Camilla Andersson, Roberto Bellasio, Bertrand Bessagnet, Roberto Bianconi, Johannes Bieser, Jørgen Brandt, Gino Briganti, Andrea Cappelletti, Gabriele Curci, Jesper H. Christensen, Augustin Colette, Florian Couvidat, Cornelis Cuvelier, Massimo D'Isidoro, Johannes Flemming, Andrea Fraser, Camilla Geels, Kaj M. Hansen, Christian Hogrefe, Ulas Im, Oriol Jorba, Nutthida Kitwiroon, Astrid Manders, Mihaela Mircea, Noelia Otero, Maria-Teresa Pay, Luca Pozzoli, Efisio Solazzo, Svetlana Tsyro, Alper Unal, Peter Wind, and Stefano Galmarini Modeled deposition of nitrogen and sulfur in Europe estimated by 14 air quality model systems: evaluation, effects of changes in emissions and implications for habitat protection Atmos. Chem. Phys., 18, 10199–10218, https://doi.org/10.5194/acp-18-10199-2018, 2018

Vautard, R., Moran, M., Solazzo, E., Gilliam, R., Volker, M., Bianconi, R., Chemel, C., Ferreira, J., Geyer, B., Hansen, A.B., Jericevic, A., Prank, M., Segers, A., Silver, J.D., Werhahn, J., Wolke, R., Rao, S.T., Galmarini, S., 2012. Evaluation of the meteorological forcing used for the Air Quality Model Evaluation International Initiative (AQMEII) air quality simulations. Atmos. Environ. 53, 38e50.

Wang, C.-H., Campell, P.C., Makar, P., Ma, S., Ivanova, I., Baek, B.H., Hung, W.-T., Moon, Z., Tang, Y., Baker, B., Saylor, S., and Tong, D., Quantifying forest canopy shading and turbulence effects on boundary layer ozone over the United States, submitted, Atmospheric Chemistry and Physics Discussions, January 31, 2025.

Wong, A. Y. H., Geddes, J. A., Tai, A. P. K., and Silva, S. J.: Importance of dry deposition parameterization choice in global simulations of surface ozone, Atmos. Chem. Phys., 19, 14365–14385, https://doi.org/10.5194/acp-19-14365-2019, 2019.

Zhang, L., Moran, M. D., Makar, P. A., Brook, J.R., and Gong, S.: Modelling gaseous dry deposition in AURAMS: a unified regional air-quality modelling system, Atmos. Environ., 36(3), 537–560, 2002. https://doi.org/10.1016/S1352-2310(01)00447-2, 2002.

https://doi.org/10.5194/egusphere-2025-1091
Preprint. Discussion started: 19 March 2025

1121

https://doi.org/10.5194/egusphere-2025-1091
Preprint. Discussion started: 19 March 2025

Table 1: Institutions in charge and the models used in AQMEII4 case studies.

Abbreviation	Modeling System (dep. scheme)	Domain	Modeling Group	Dry Deposition Scheme	LU for Dry Deposition Scheme
NA1 (10700)	WRF/CMAQ (M3Dry)	NA	U.S. EPA	M3Dry	MODIS
NA2 (10701)	WRF/CMAQ (STAGE)	NA	U.S. EPA	STAGE	AQMEII4 (mapped from MODIS)
NA3 (10703)	GEM-MACH (Base)	NA	Environment and Climate Change Canada	Wesely	Robichaud (Robichaud et al. 2020)
NA4 (10704)	GEM-MACH (Zhang)	NA	Environment and Climate Change Canada	Zhang	Zhang et al. (2003)
NA5 (10705)	GEM-MACH (Ops)	NA	Environment and Climate Change Canada	Wesely	Robichaud (Robichaud et al. 2020)
NA6 (10702)	WRF-Chem (RIFS)	NA	Research Center for Sustainability (RIFS)	Wesely	USGS24
NA7 (10708)	WRF-Chem (UPM)	NA	Technical University of Madrid (UPM)	Wesely	USGS24
NA8 (10709)	WRF-Chem (NCAR)	NA	National Center for Atmospheric Research / Yonsei University	Wesely	USGS24
EU1 (10702)	WRF-Chem (RIFS)	EU	Research Center for Sustainability (RIFS)	Wesely	CORINE 33
EU2 (10708)	WRF-Chem (UPM)	EU	Technical University of Madrid (UPM)	Wesely	USGS24
EU3 (10707)	LOTOS/EUROS	EU	TNO	DEPAC	Van Zanten, M. C., 2010.
EU4 (10710)	WRF/CMAQ (STAGE)	EU	University of Hertfordshire	STAGE	MODIS + extended urban

https://doi.org/10.5194/egusphere-2025-1091
Preprint. Discussion started: 19 March 2025

Table 2: NA case. For all available combinations of models $\binom{m}{n}$ analysed, the table presents those that produce the minimum errors (blue columns) as well as all other combinations that fall within 10% of that minimum error (yellow and orange columns). The minimum RMSE of 3.77 ppb is achieved by the second order ($\binom{8}{2}$, all combinations of 2 models out of 8) combination of WRF/CMAQ (STAGE) and GEM-MACH (Ops) as well as the third order ($\binom{8}{3}$, all combinations of 3 models out of 8) combination of WRF/CMAQ (STAGE), GEM-MACH (Base), and GEM-MACH (Ops) . The combinations with the second lowest RMSE are shown in the orange columns. The frequency column shows the number of times each model was part of an ensemble weighted by the number of ensembles considered.

MODEL	Model code	Frequency (%)	Order of Model Combination										
			1		2				3			4	
WRF/CMAQ (M3Dry)	NA1 (10700)	36.4				X				X	X	X	
WRF/CMAQ (STAGE)	NA2 (10701)	54.5			X		X		X	X		X	X
GEM-MACH (Base)	NA3 (10703)	63.6		X			X	X	X		X	X	X
GEM-MACH (Zhang)	NA4 (10704)												
GEM-MACH (Ops)	NA5 (10705)	81.8	X		X	X		X	X	X	X	X	X
WRF-Chem (RIFS)	NA6 (10702)	9.1											X
WRF-Chem (UPM)	NA7 (10708)												
WRF-Chem (NCAR)	NA8 (10709)												
RMSE (ppb)			3.90	3.95	3.77	3.86	4.02	3.83	3.77	4.04	3.83	3.93	4.10

Table 3: Same as Table 2a for the EU case

MODEL	Model code	Freq. (%)	Order of Model Combination				
			2		3		4
WRF-Chem (RIFS)	EU1 (10702)	60	X		X		X
WRF-Chem (UPM)	EU2 (10708)	40				X	X
LOTOS/EUROS	EU3 (10707)	100	X	X	X	X	X
WRF/CMAQ (STAGE)	EU4 (10710)	80		X	X	X	X
RMSE (ugm^{-3})			**7.51**	8.15	7.92	8.11	8.17

https://doi.org/10.5194/egusphere-2025-1091
Preprint. Discussion started: 19 March 2025

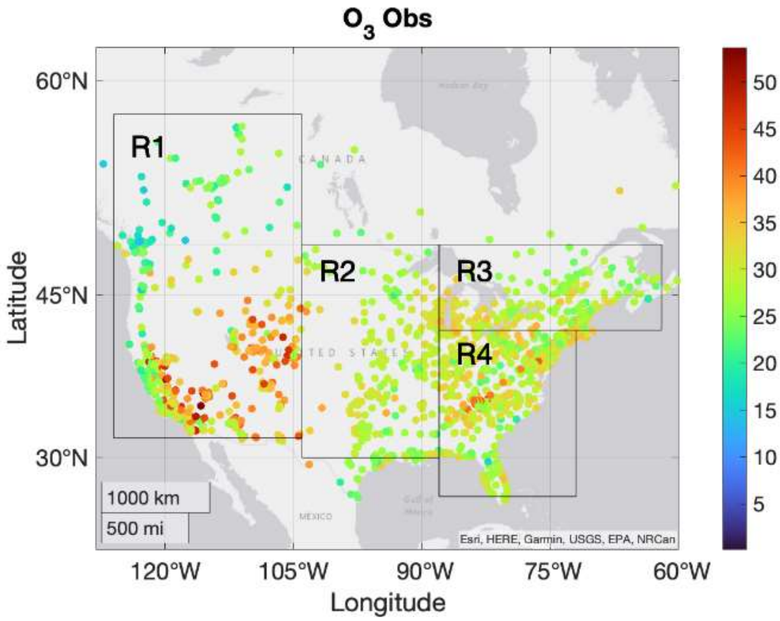

(a)

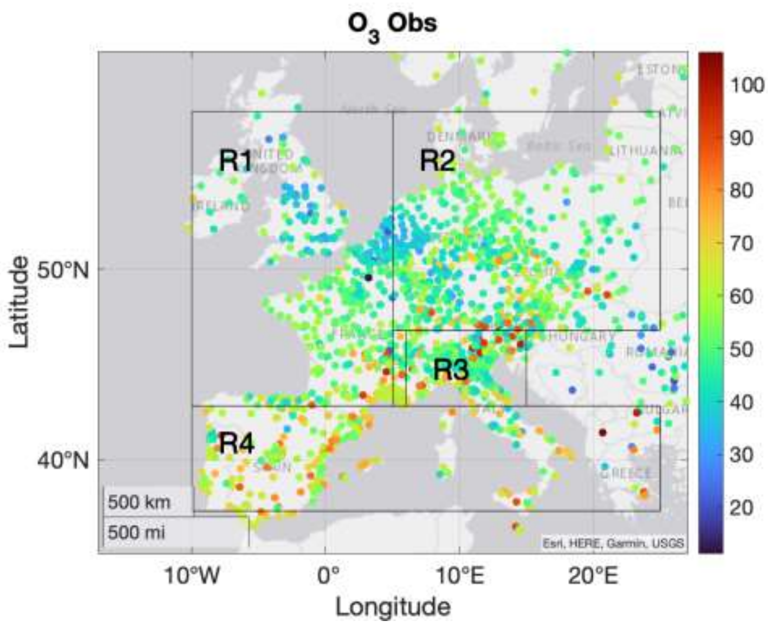

(b)

1136

1137 **Figure 1**: Annual average of ozone at all available monitoring stations in North America for 2016 (a) [ppb]
1138 and Europe for 2010 (b) [$\mu g\ m^{-3}$].

https://doi.org/10.5194/egusphere-2025-1091
Preprint. Discussion started: 19 March 2025

https://doi.org/10.5194/egusphere-2025-1091
Preprint. Discussion started: 19 March 2025

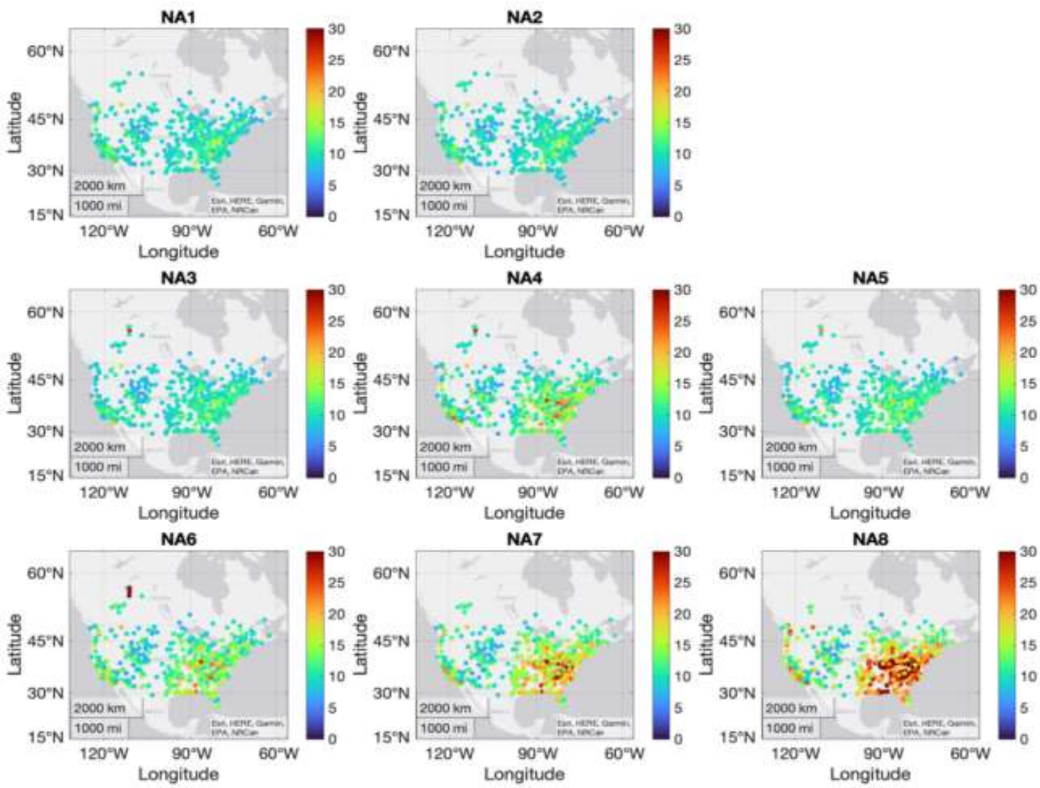

1141 **Figure 2**: Individual model ozone RMSE calculated over the whole year (2016) over NA. From NA1 through
1142 NA8: WRF/CMAQ (M3Dry), WRF/CMAQ (STAGE), GEM-MACH (Base), GEM-MACH (Zhang), GEM-MACH
1143 (Ops), WRF-Chem (RIFS), WRF-Chem (UPM), and WRF-Chem (NCAR). Units are in ppb.

https://doi.org/10.5194/egusphere-2025-1091
Preprint. Discussion started: 19 March 2025

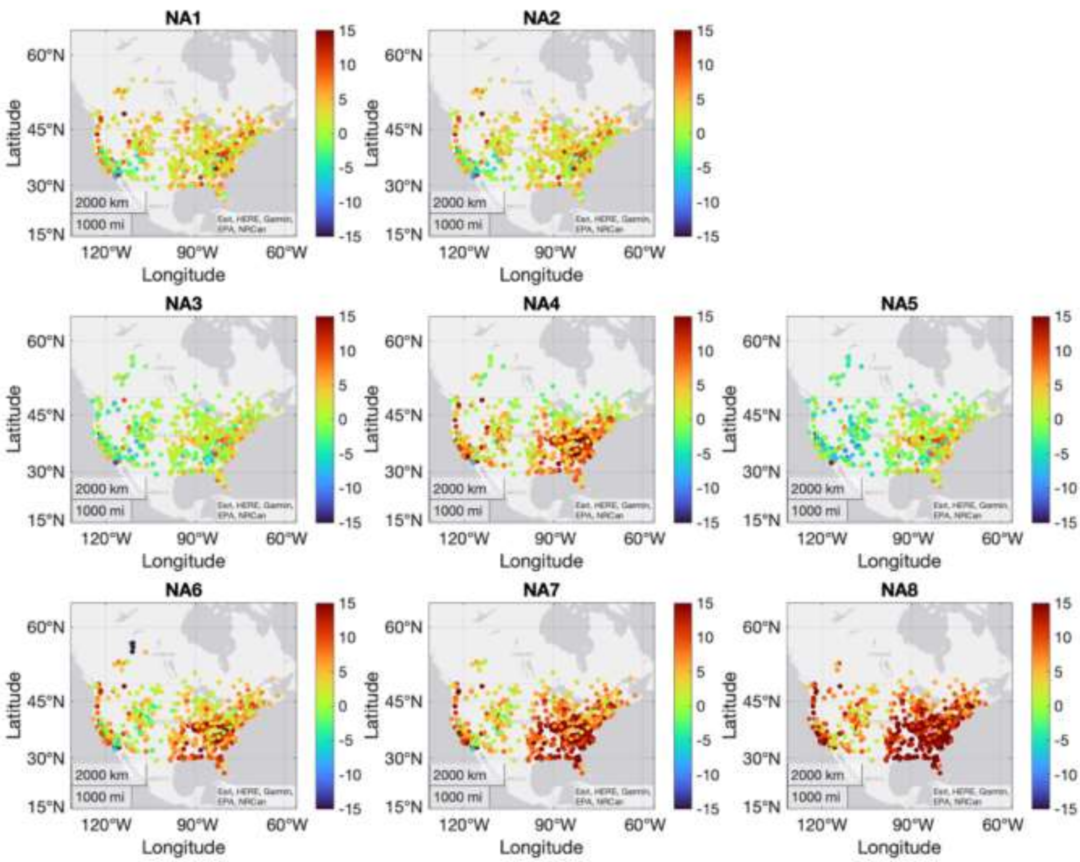

1145 **Figure 3**: Individual model ozone MB calculated over the whole year (2016) over NA. From NA1 through
1146 NA8: WRF/CMAQ (M3Dry), WRF/CMAQ (STAGE), GEM-MACH (Base), GEM-MACH (Zhang), GEM-MACH
1147 (Ops), WRF-Chem (RIFS), WRF-Chem (UPM), and WRF-Chem (NCAR). Units are in ppb.

1148

1149

https://doi.org/10.5194/egusphere-2025-1091
Preprint. Discussion started: 19 March 2025

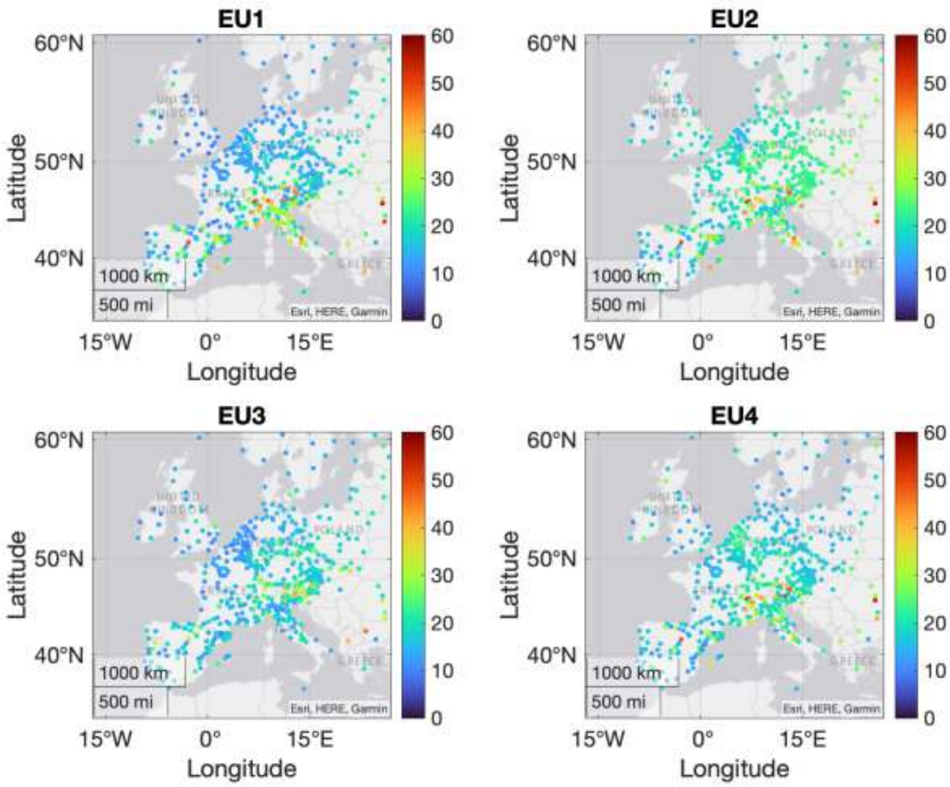

Figure 4: Individual model ozone RMSE calculated over the whole year (2010) over EU. From EU1 through EU4: WRF-Chem (RIFS), WRF-Chem (UPM), LOTOS/EUROS, WRF/CMAQ (STAGE). Units are in µg/m^3. Colour bars are set to twice the range used in Figure 2 to allow for a visual comparison across continents, accounting for the conversion factor of 1.96 between the different units.

https://doi.org/10.5194/egusphere-2025-1091
Preprint. Discussion started: 19 March 2025

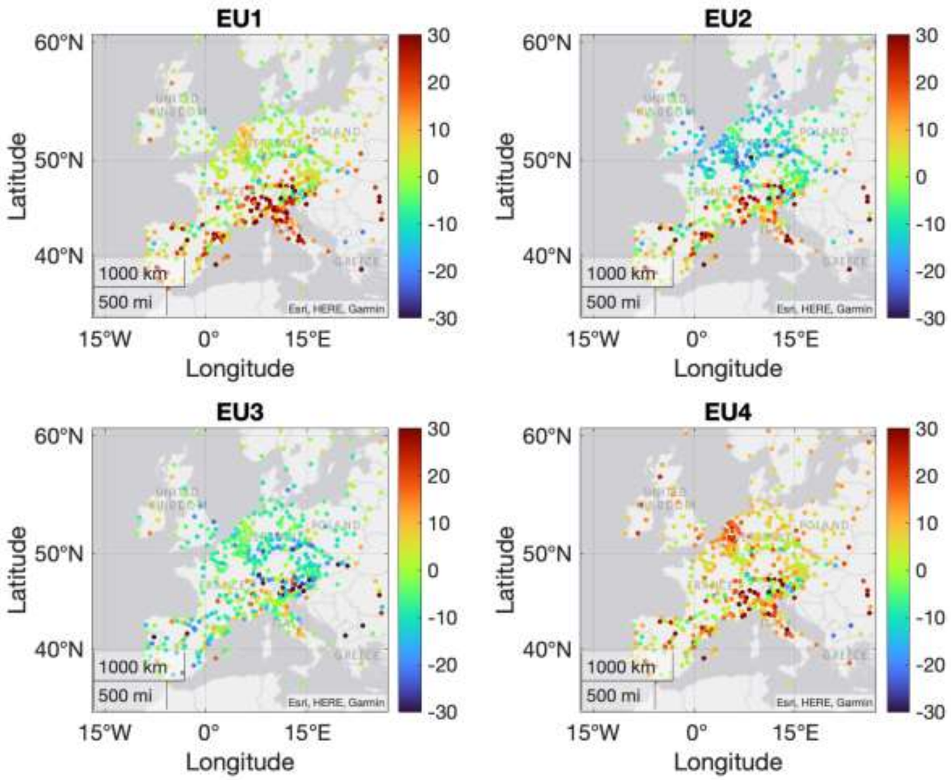

Figure 5: Individual model ozone MB calculated over the whole year (2010) over EU. From EU1 through EU4: WRF-Chem (RIFS), WRF-Chem (UPM), LOTOS/EUROS, WRF/CMAQ (STAGE). Units are in μg/m^3. Colour bars are set to twice the range used in Figure 2b to allow for a visual comparison across continents, accounting for the conversion factor of 1.96 between the different units.

https://doi.org/10.5194/egusphere-2025-1091
Preprint. Discussion started: 19 March 2025

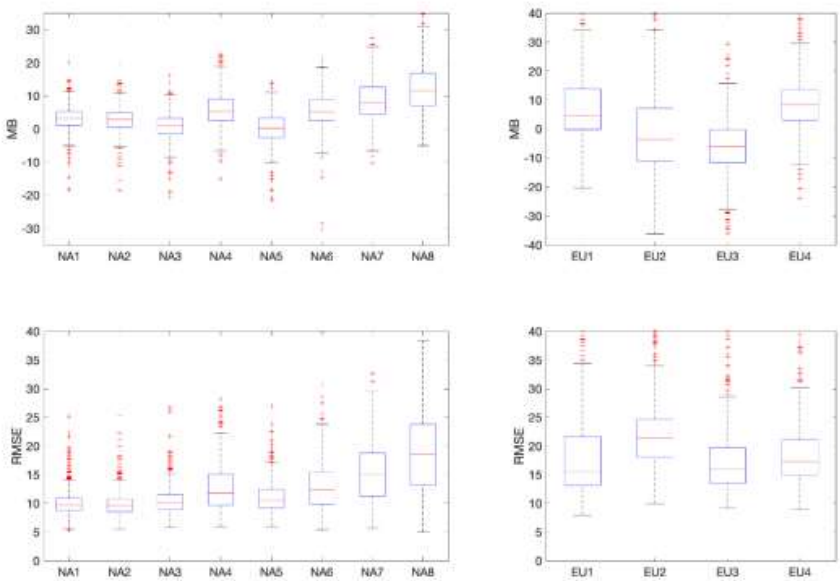

(a) (b)

Figure 6: Individual model ozone MB (top panels) and RMSE (bottom panels) calculated over the whole year over NA (a) and EU (b). NA case units: ppb, EU: µg/m^3

https://doi.org/10.5194/egusphere-2025-1091
Preprint. Discussion started: 19 March 2025

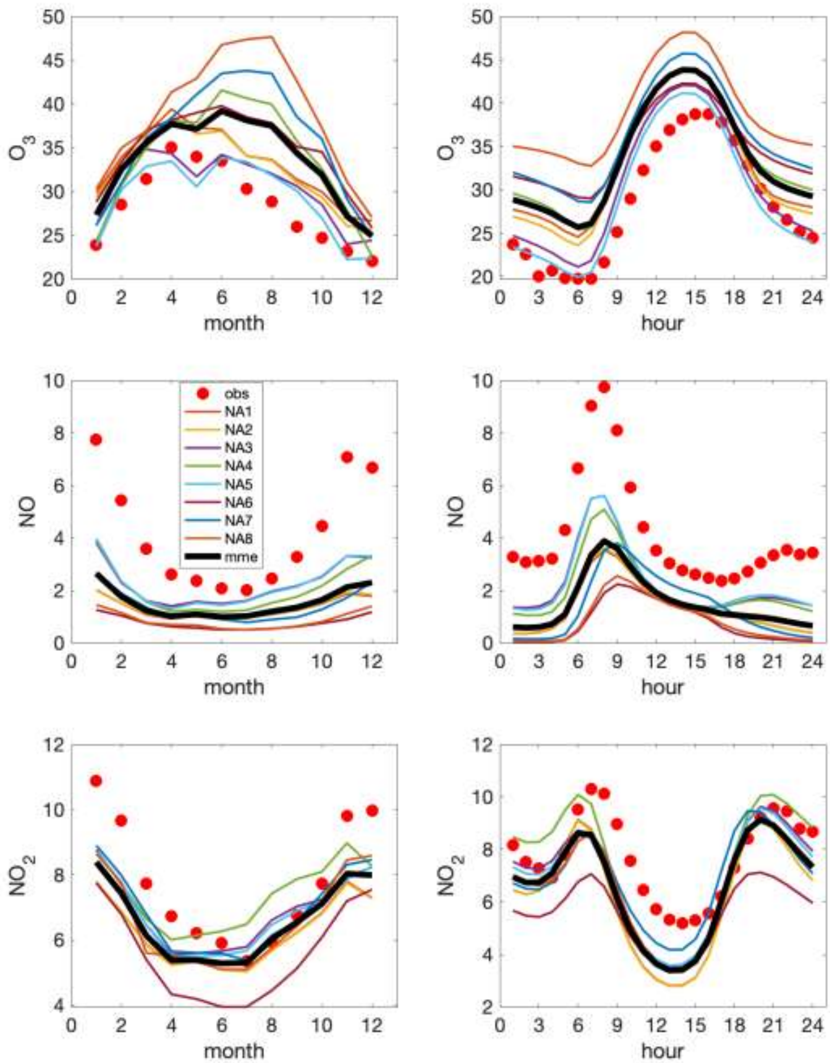

Figure 7: Average monthly (left panels) and diurnal (right panels) cycles of ozone, NO, and NO_2 [ppb] for the 2016 NA case study. Thin coloured lines: models; red dots: observations; black line: multi-model mean.

https://doi.org/10.5194/egusphere-2025-1091
Preprint. Discussion started: 19 March 2025

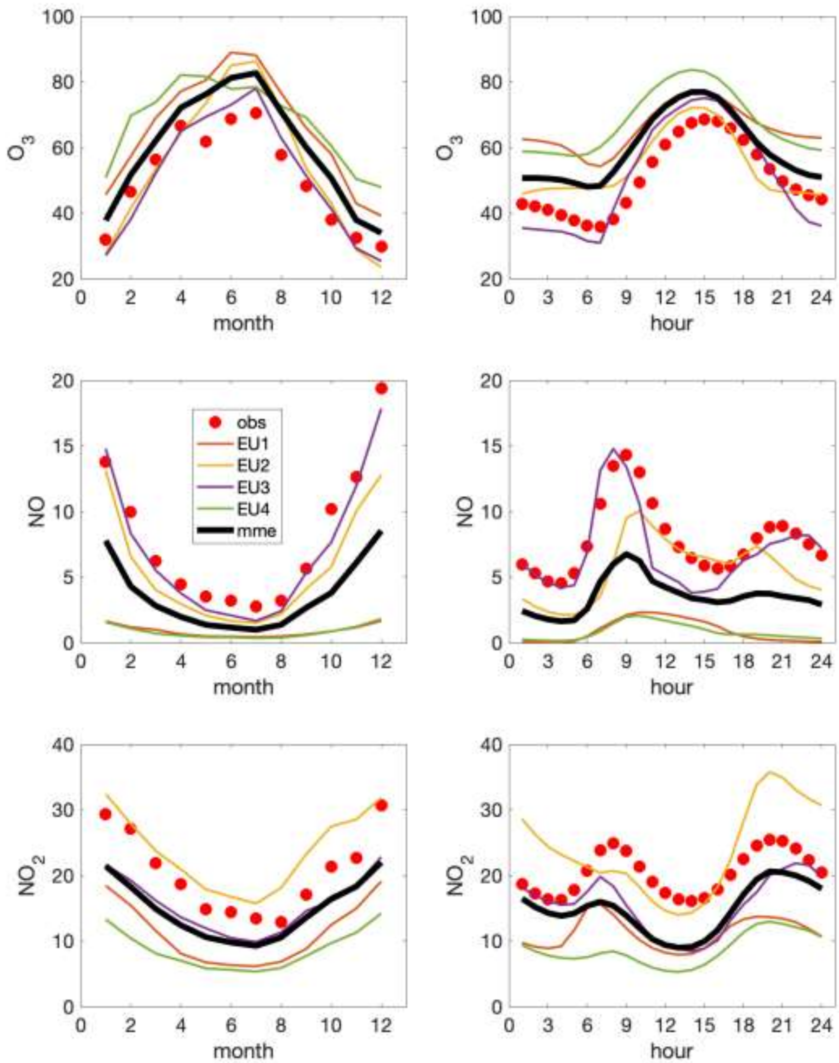

1177

1178 **Figure 8**: Average monthly (left panels) and diurnal (right panels) cycles of ozone, NO, and NO_2 [µg m^{-3}] for

1179 the 2010 EU case study. Thin coloured lines: models; red dots: observations; black line: multi-model mean.

1180

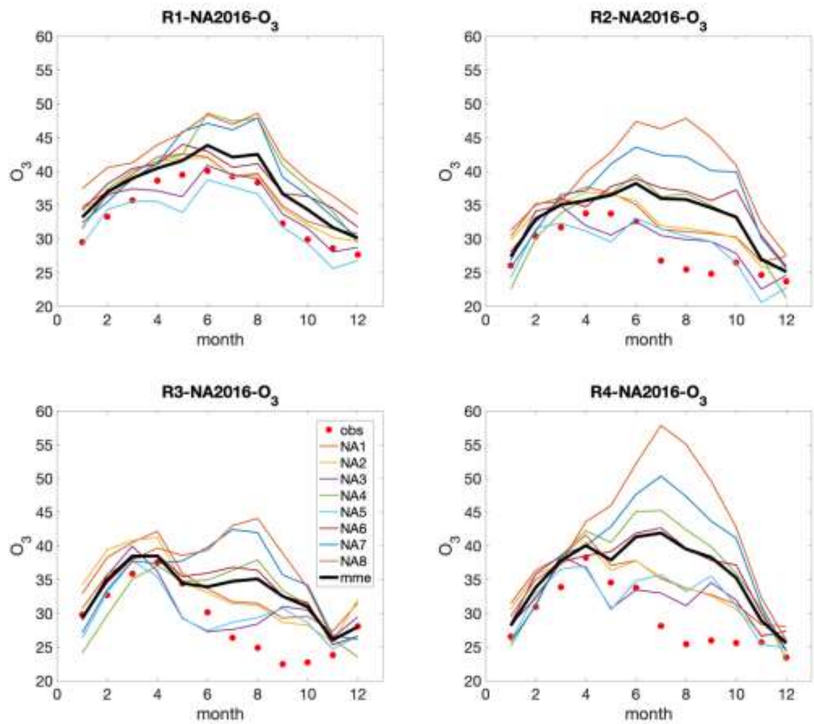

1181

1182

1183 **Figure 9**: Monthly average cycles of O_3 concentrations in [ppb] as calculated in sub-regions R1-R4 over the
1184 NA domain. Thin coloured lines: models; red dots: observations; black line: multi-model mean.

1185

https://doi.org/10.5194/egusphere-2025-1091
Preprint. Discussion started: 19 March 2025

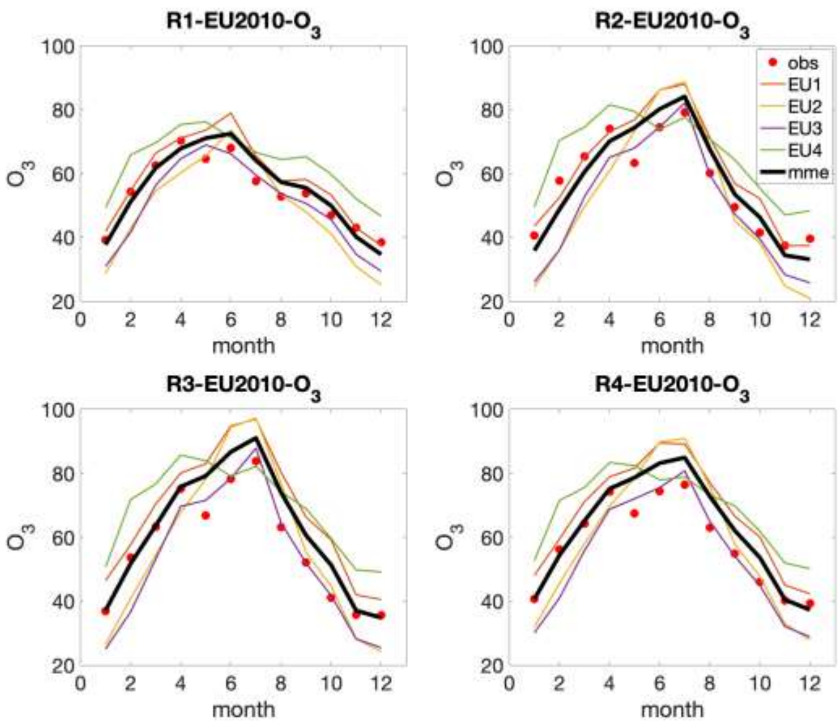

1186

1187 **Figure 10**: Monthly average cycles of O_3 concentrations in [µg m^{-3}] as calculated in sub-regions R1-R4 over
1188 the EU domains. Thin coloured lines: models; red dots: observations; black line: multi-model median.

1189

https://doi.org/10.5194/egusphere-2025-1091
Preprint. Discussion started: 19 March 2025

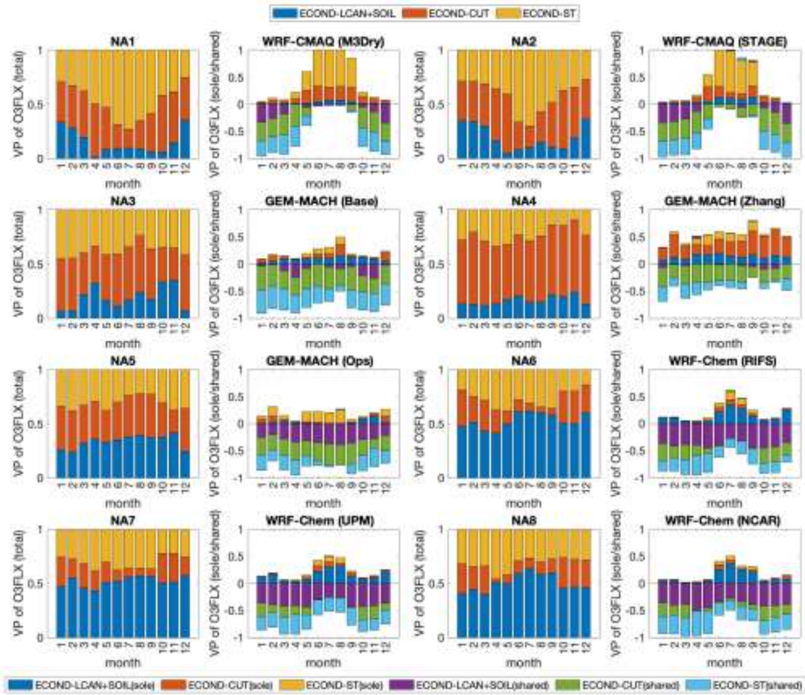

Figure 11: NA case study at 1544 shared cells covered by at least 85% of needle-leaf forest. Panels in 1st and 3rd column: variance partition (VP) of ozone dry deposition flux into the individual importance (i.e. total effect) of (1) lower canopy and soil effective fluxes combined in one factor, (2) cuticular effective flux and (3) stomatal effective flux. Panels in 2nd and 4th column: Split of the individual importance of the effective fluxes into sole and shared contributions. The shared effects are displayed with negative numbers. For the sake of making the pictures easier to read, the explicit names of the modelling systems are reported in the figure.

https://doi.org/10.5194/egusphere-2025-1091
Preprint. Discussion started: 19 March 2025

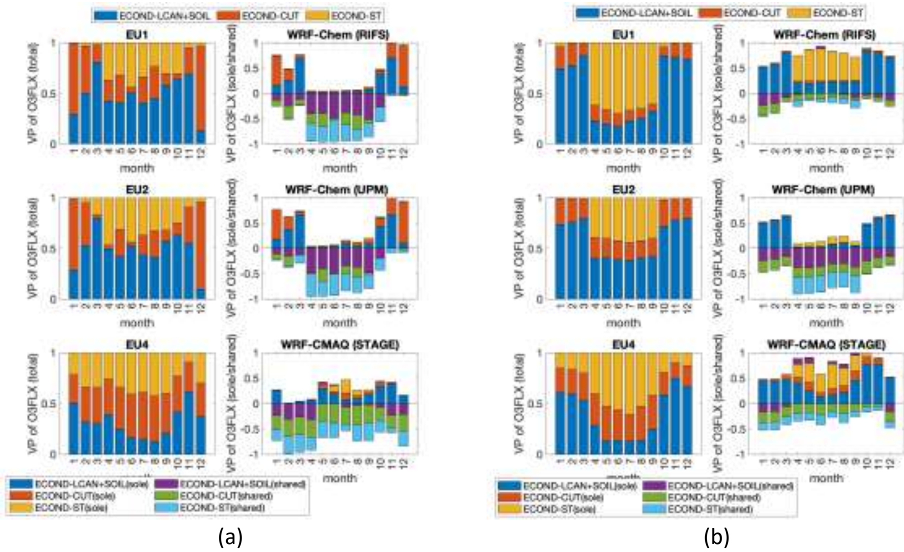

Figure 12: (a) EU case study at 2531 shared cells covered by at least 85% of needle-leaf forest. Panels in 1st column: variance partition (VP) of ozone dry deposition flux into the individual importance (i.e. total effect) of (1) lower canopy and soil effective fluxes combined in one factor, (2) cuticular effective flux and (3) stomatal effective flux. Panels in 2nd column: Split of the individual importance of the effective fluxes into sole and shared contributions. The shared effects are displayed with negative numbers. For the sake of making the pictures easier to read, the explicit names of the modelling systems are reported in the figure. (b) Same as a) but at the location of ozone receptors in EU (1551 shared cells).

https://doi.org/10.5194/egusphere-2025-1091
Preprint. Discussion started: 19 March 2025

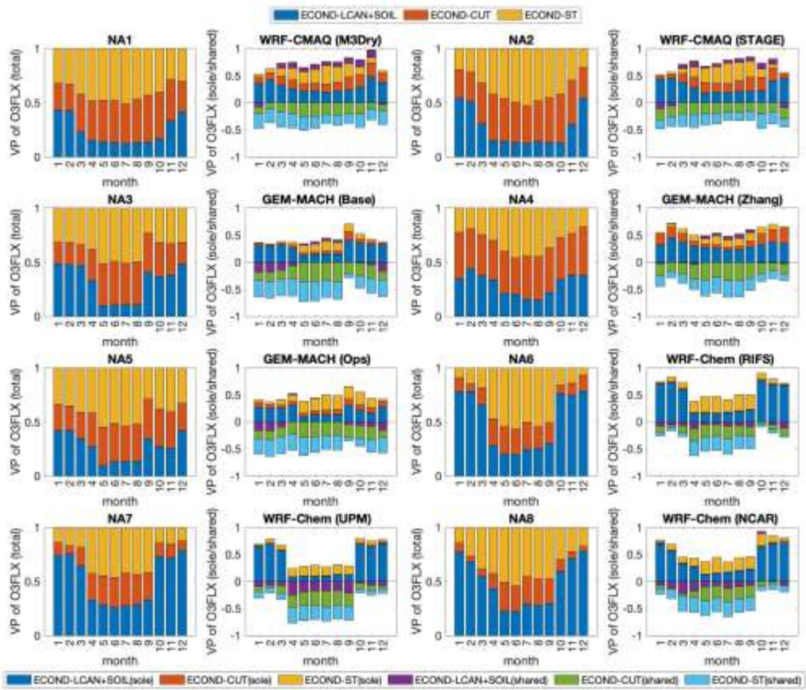

Figure 13: Same as 7 but at the location of ozone Receptors in NA (1551 shared cells).

https://doi.org/10.5194/egusphere-2025-1091
Preprint. Discussion started: 19 March 2025

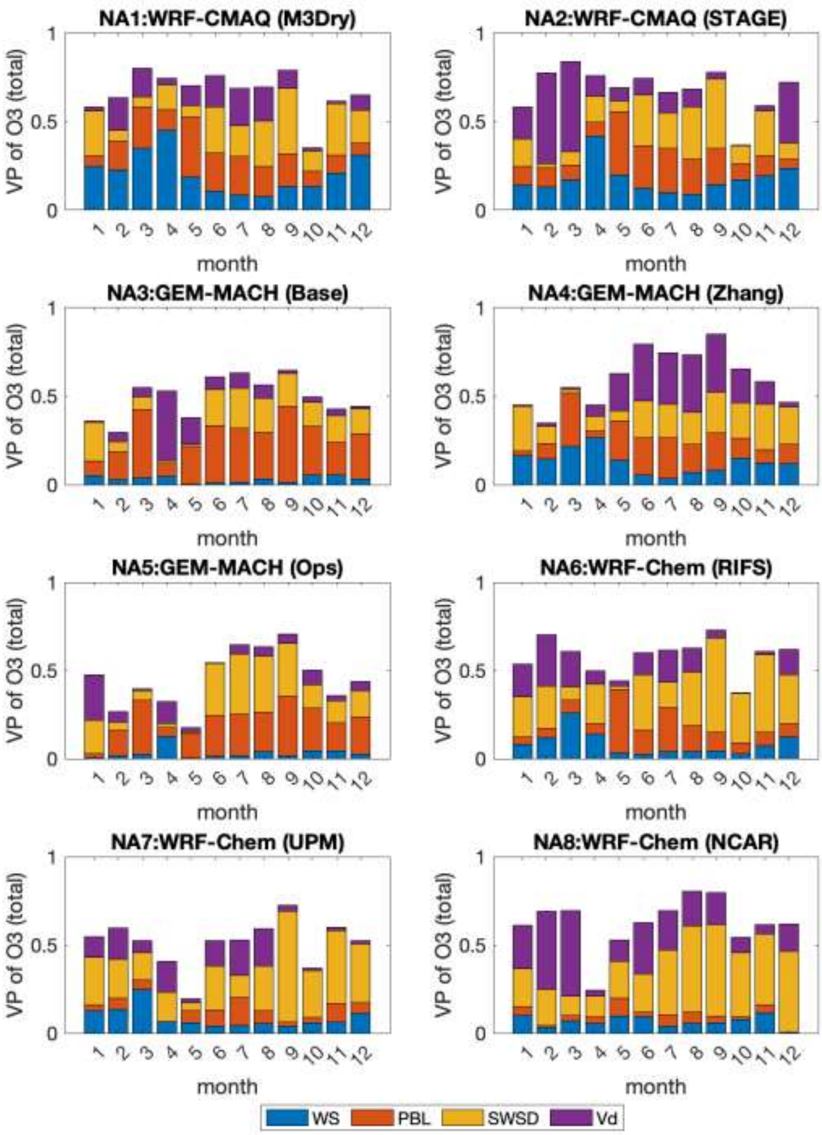

Figure 14: NA case study at 1544 shared cells covered by at least 85% of needle-leaf forest. Variance partition (VP) of ozone concentration for each model into the individual importance (i.e. total effect) of wind speed, PBL height, solar radiation, and deposition velocity. For the sake of making the pictures easier to read, the explicit names of the modelling systems are reported in the figure.

https://doi.org/10.5194/egusphere-2025-1091
Preprint. Discussion started: 19 March 2025

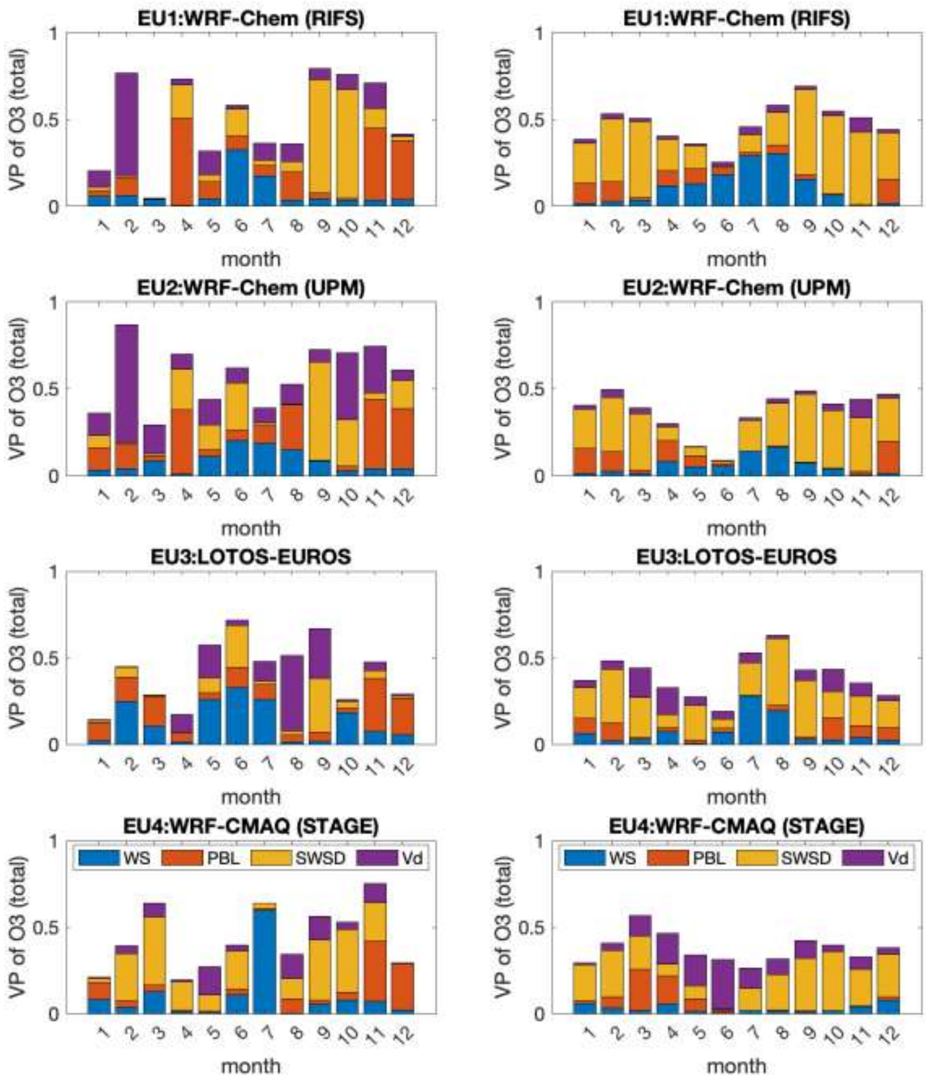

(a) (b)

Figure 15: (a) EU case study at 2531 shared cells covered by at least 85% of needle-leaf forest. Variance partition (VP) of ozone concentration for each model into the individual importance (i.e. total effect) of wind speed, PBL height, solar radiation, and deposition velocity. For the sake of making the pictures easier to read, the explicit names of the modeling systems are reported in the figure. (b) Same as a) but at the location of the ozone receptors in EU (1551 shared cells).

https://doi.org/10.5194/egusphere-2025-1091
Preprint. Discussion started: 19 March 2025

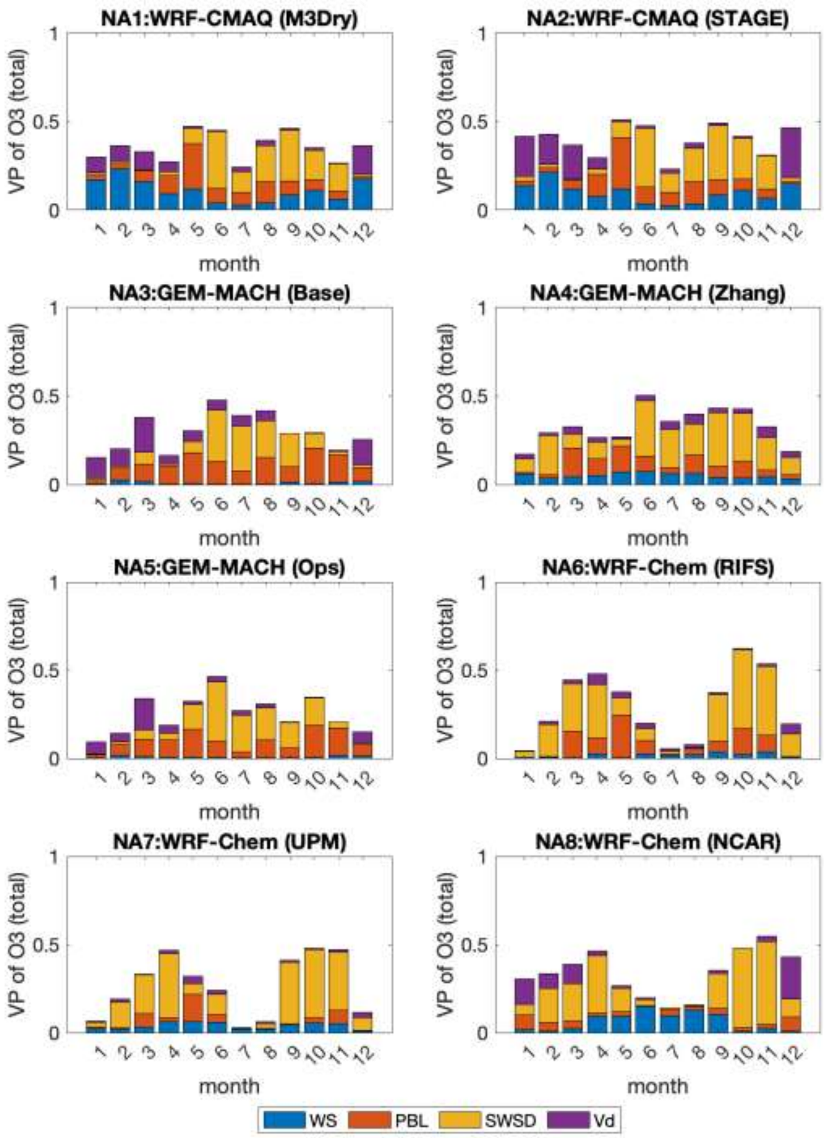

Figure 16: Same as 10 but at the location of ozone receptors in NA (1551 shared cells).

https://doi.org/10.5194/egusphere-2025-1091
Preprint. Discussion started: 19 March 2025

(a)

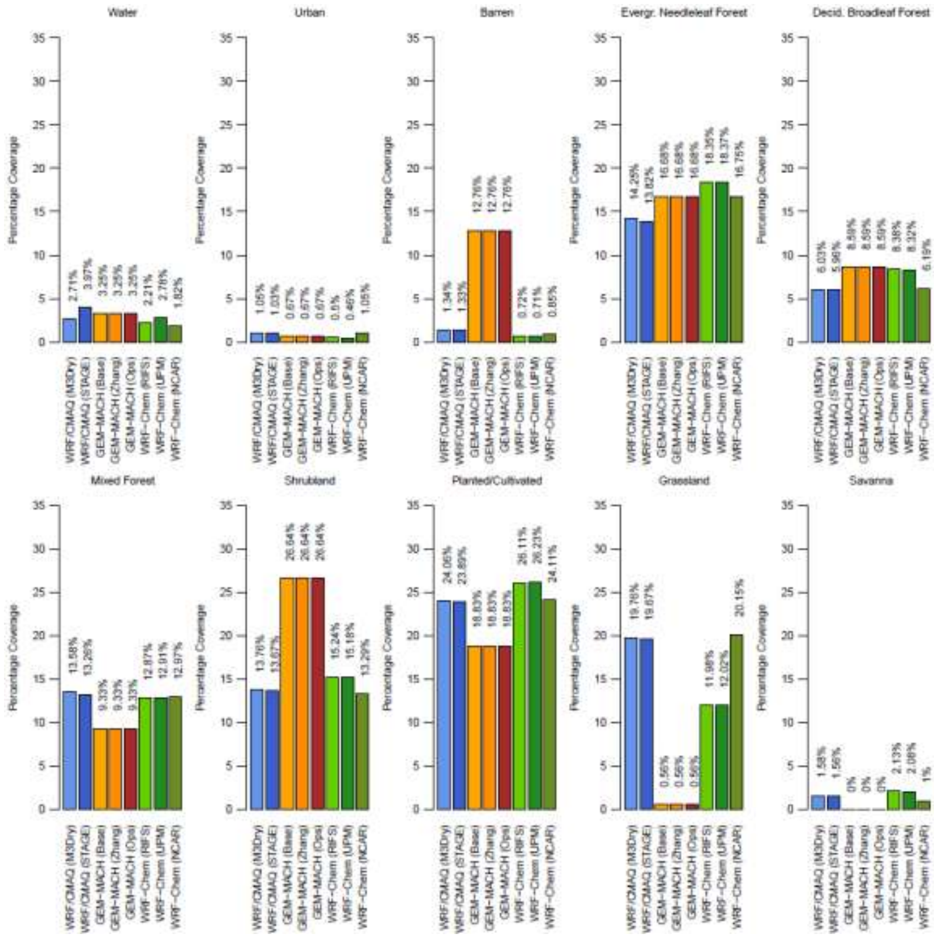

(a)

https://doi.org/10.5194/egusphere-2025-1091
Preprint. Discussion started: 19 March 2025

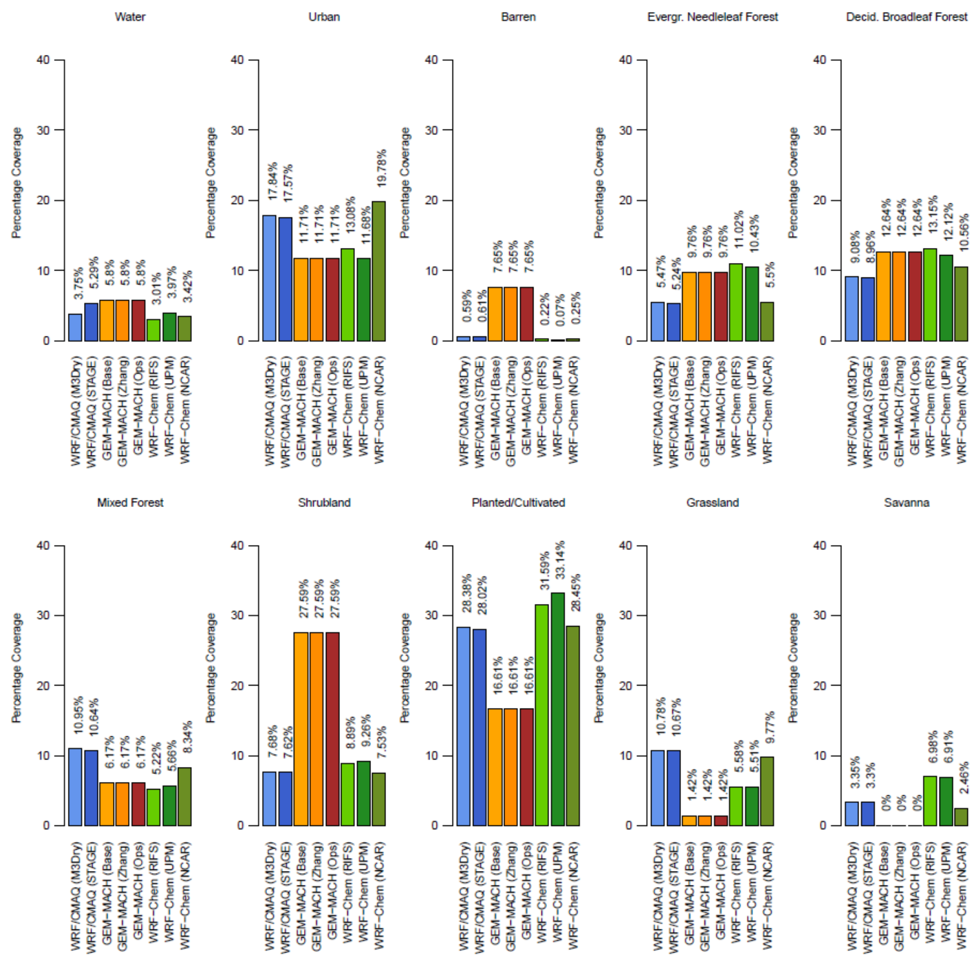

(b)

(b)

Figure 17: (a) Fraction of entire NA common domain (excl. grid cells dominated by water, i.e. water fraction > 0.5) covered by each LU type. (b) Fraction of all grid cells corresponding to O3 receptor locations covered by each LU type.